

A Dissertation  
entitled  
Quantum Theory of Many Bose Atom Systems

by  
Imran Khan

Submitted as partial fulfillment of the requirements for the  
Doctor of Philosophy Degree in Physics

---

Advisor: Dr. Bo Gao

---

Graduate School

The University of Toledo  
December 2007



An Abstract of  
Quantum Theory of Many Bose Atom Systems

Imran Khan

Submitted in partial fulfillment  
of the requirements for the  
Doctor of Philosophy Degree in Physics

The University of Toledo  
December 2007

This dissertation describes some of the efforts involved in developing a systematic understanding of Quantum many-atom systems with real atomic interactions. Specifically, we develop and apply a non-perturbative Quantum theory of many-atom systems under a strong long-range interaction. A non-perturbative theory is necessary because the perturbation method cannot adequately describe many-atom systems with strong interactions, especially if the interactions are strong enough to form bound states. The long-range behaviour is of special significance because it determines the universal behaviour of an atomic system.

In order to calculate the equation of state, at the Van der Waals length scale, a variance minimized variational Monte Carlo (VMVMC) method is developed. Unlike the standard Monte Carlo method, the VMVMC method minimizes the variance of the energy instead of the energy itself. Minimizing the energy is only suitable for the true ground state of a system; many-atom systems represent highly excited states, so, therefore it is not suitable to minimize the energy and instead the variance is minimized. This concept has been developed by Dr. Gao and it has a wider range of

applicability than results based on mean field theory or perturbation theory.

Results are presented for few and many-atom systems with or without a trap and for both positive and negative scattering lengths.

## Acknowledgments

I would like to thank my advisor, Dr. Bo Gao, for his unlimited patience, guidance and support. I would like to thank my committee members for their patience and dedication in reading and correcting my dissertation. I would also like to thank my friends, David Horne and Stephanie Torok, for injecting some humour into the last few years. Finally I'd like to acknowledge the tremendous support offered by the faculty, staff and students of the department of Physics and Astronomy, especially Dr. Richard Irving, Bob Lingohr, Yujun Chen, Sue Hickey, Mike Brown and Willie Brown.

Dedicated to my dear wife, Aasma, and my new family; uncle Khalid, auntie Rashda, brother Rehan and sister Henna, whose love and encouragement in my final year has been invaluable.

# Contents

<b>Abstract</b>	<b>ii</b>
<b>Acknowledgments</b>	<b>iv</b>
<b>Contents</b>	<b>v</b>
<b>List of Figures</b>	<b>viii</b>
<b>List of Tables</b>	<b>xi</b>
<b>1 Introduction</b>	<b>1</b>
1.1 Statement of Problem . . . . .	1
1.2 Dissertation Breakdown . . . . .	2
<b>2 Background</b>	<b>4</b>
2.1 Many-Body systems . . . . .	4
2.1.1 Statistical Physics . . . . .	5
2.1.2 Quantum Mechanics . . . . .	9
2.1.3 Many-Atom Interactions . . . . .	10
2.1.4 Tools for Investigating Many-Atom Systems . . . . .	13

2.2	Monte Carlo Methods . . . . .	15
2.2.1	Variational Monte Carlo . . . . .	15
2.3	Quantum Defect Theory . . . . .	18
2.4	Bose-Einstein Condensation . . . . .	20
2.4.1	Historical . . . . .	20
2.4.2	Previous BECs . . . . .	21
2.5	Dilute Bose Gases . . . . .	23
2.5.1	Cooling . . . . .	23
<b>3</b>	<b>Many Atom Quantum Theory</b>	<b>27</b>
3.1	Variational Method . . . . .	27
3.2	Variational Monte Carlo . . . . .	28
3.2.1	Local Energy . . . . .	28
3.2.2	Trial Wavefunction . . . . .	31
3.2.3	Variance Minimisation . . . . .	33
3.2.4	Universal equation of state at the Van der Waals length scale for $N$ Bose atoms in a symmetric harmonic trap . . . . .	36
<b>4</b>	<b>Results</b>	<b>40</b>
4.1	Testing . . . . .	40
4.1.1	Hard Spheres in a Trap . . . . .	40
4.1.2	Homogeneous Bose System . . . . .	42
4.2	Few Atoms in a Trap . . . . .	47
4.2.1	Positive Scattering Length . . . . .	50

4.2.2	Negative Scattering Length . . . . .	54
4.3	Homogeneous Bose Gas . . . . .	55
4.4	Excited states . . . . .	61
<b>5</b>	<b>Conclusions</b>	<b>71</b>
5.1	Atoms in a trap . . . . .	71
5.2	Homogeneous Bose Gas . . . . .	73
5.3	Excited States . . . . .	73
5.4	Further Work . . . . .	74
<b>A</b>	<b>VMVMC Class Structure</b>	<b>75</b>
<b>B</b>	<b>Data Tables</b>	<b>77</b>
B.1	Hard Spheres In a Trap . . . . .	77
B.2	Atoms in a Trap . . . . .	79
B.2.1	Positive scattering length . . . . .	79
B.2.2	Negative scattering length . . . . .	79
<b>C</b>	<b>Further Comments on Implementation</b>	<b>83</b>

# List of Figures

2-1	An example of the real interaction potential between atoms. . . . .	7
2-2	Van der Waals potential. . . . .	8
2-3	The behaviour of particles above and below $T_c$ . . . . .	22
2-4	Experimental setup. . . . .	24
2-5	Left: Just before the BEC. Centre: Just after the appearance of the condensate. Right: After further evaporation - nearly a pure condensate. . . . .	25
4-1	A comparison of the DMC[1] and VMC values for two hard spheres in a symmetric harmonic trap. . . . .	43
4-2	A comparison of the DMC[1] and VMC values for $N = 3$ (lower curve) and $N = 5$ (upper curve) hard spheres in a symmetric harmonic trap. . . . .	44
4-3	A comparison of the DMC[1] and VMC values for $N = 10$ (lower curve) and $N = 20$ (upper curve) hard spheres in a symmetric harmonic trap. . . . .	45
4-4	A comparison of the DMC[2] and VMC values for hard spheres in a homogeneous system. . . . .	48

4-5	The universal equation of state for three atoms in a symmetric harmonic trap as a function of $a_0/a_{ho}$ , compared to the DMC results of Blume and Greene for hard spheres [1]. . . . .	50
4-6	The parameter $\gamma$ , characterizing the long-range atom-atom correlation, for three atoms in a symmetric harmonic trap, as a function of $a_0/a_{ho}$ .	52
4-7	The universal equation of state for five atoms in a symmetric harmonic trap as a function of $a_0/a_{ho}$ , compared to the DMC results of Blume and Greene for hard spheres [1]. . . . .	53
4-8	The parameter $\gamma$ , characterizing the long-range atom-atom correlation, for five atoms in a symmetric harmonic trap, as a function of $a_0/a_{ho}$ .	54
4-9	The universal equation of state for three atoms in a symmetric harmonic trap as a function of $a_0/a_{ho}$ , with negative scattering length. . . . .	56
4-10	The universal equation of state for five atoms in a symmetric harmonic trap as a function of $a_0/a_{ho}$ , with negative scattering length. . . . .	57
4-11	Positive scattering length. . . . .	59
4-12	Negative scattering length. . . . .	60
4-13	The universal spectrum at length scale $\beta_6$ for two Bose atoms in a symmetric harmonic trap as a function of $a_0/a_{ho}$ for $\beta_6/a_{ho} = 0.001$ . Solid line: results from a multiscale QDT [3]. Symbols: results of VMVMC. . . . .	68
4-14	The same as Fig. 4-13 except for $\beta_6/a_{ho} = 0.1$ . . . . .	69

4-15	A comparison of the spectra for two different values of $\beta_6/a_{ho}$ , illustrating the shape-dependent correction that becomes more important for greater values of $\beta_6/a_{ho}$ and for more highly excited states. . . .	70
C-1	Energy per particle for three atoms in a trap, with $a_0/a_{ho} = 0.0866$ and $\beta_6/a_{ho} = 0.001$ , as a function of the number of $s$ wave bound states supported by a HST effective potential. . . . .	85

# List of Tables

B.1	Data of energy per particle, in units of $\hbar\omega$ , for two hard spheres in a symmetric harmonic trap. The number in the parenthesis represents the variance in the last digit. . . . .	77
B.2	Data of energy per particle, in units of $\hbar\omega$ , for three and five hard spheres in a symmetric harmonic trap. The number in the parenthesis represents the variance in the last digit. . . . .	78
B.3	Data of energy per particle, in units of $\hbar\omega$ , for ten and twenty hard spheres in a symmetric harmonic trap. The number in the parenthesis represents the variance in the last digit. . . . .	78
B.4	Data of energy per particle for a homogeneous Bose gas, in units of $\hbar^2/2ma^2$ . The number in the parenthesis represents the variance in the last digit. . . . .	79
B.5	Data of energy per particle, in units of $\hbar\omega$ , for three atoms in a symmetric harmonic trap. The number in the parenthesis represents the variance in the last digit. . . . .	80

B.6	Data of energy per particle, in units of $\hbar\omega$ , for five atoms in a symmetric harmonic trap. The number in the parenthesis represents the variance in the last digit. . . . .	80
B.7	Values of the variational parameter $\gamma$ , from Eq.( 3.17) for three particles in a symmetric harmonic trap. . . . .	81
B.8	Values of the variational parameter $\gamma$ , from Eq.( 3.17) for five particles in a symmetric harmonic trap. . . . .	81
B.9	Negative scattering length data of energy per particle, in units of $\hbar\omega$ , for three atoms in a symmetric harmonic trap. The number in the parenthesis represents the variance in the last digit. . . . .	82
B.10	Negative scattering length data of energy per particle, in units of $\hbar\omega$ , for five atoms in a symmetric harmonic trap. The number in the parenthesis represents the variance in the last digit. . . . .	82

# Chapter 1

## Introduction

### 1.1 Statement of Problem

The problem under investigation is to develop a non-perturbative quantum many-atom theory under a long-range interaction. Previous work in many-atom quantum systems has been limited to weak coupling and/or low density regimes. Weak coupling is characterized by  $\rho a_0^3 \ll 1$ , where  $\rho = N/V$  and  $a_0$  is the s-wave scattering length. Low densities are characterized by  $\rho \beta_6^3 \ll 1$ , where,  $\beta_6 = (mC_6/\hbar^2)^{1/4}$ , is the length scale associated with the Van der Waals interaction ( $-C_6/r^6$ ) between two atoms. As a consequence of these limitations there have been no general microscopic quantum theories of gases or liquids (beyond liquid Helium).

However, with the development of the angular-momentum-insensitive quantum-defect theory (AQDT) for diatomic systems [4, 5, 6] one may obtain a new understanding of atomic systems. This new framework has allowed for the investigation of universal behaviour at different length scales in quantum many-atom systems. In

particular it has allowed one to understand systems which go beyond weak coupling and allow for investigations of high densities,  $\rho\beta_6^3 \sim 10$ .

The ideas developed in this work are applied to the gaseous atomic Bose-Einstein Condensate (BEC) state. The universal equation of state at the Van der Waals length scale [B. Gao, J. Phys. B **37**, L227 (2004)] for  $N$  Bose atoms in a trap and the atomic homogeneous system is computed.

## 1.2 Dissertation Breakdown

Chapter 2 introduces some important background ideas in atomic physics and field of atomic physics overall. The chapter discusses previous ideas and mathematical methods used to understand many-atom behaviour such as the Lee-Huang-Yang (LHY) equation. The importance of universal behaviour is discovered alongside the importance of the equation of state. There is also a brief introduction to the idea of Quantum defect theory (QDT) and its important role in atomic physics. Finally there is a summary of Bose-Einstein condensation in dilute atomic gases which is one of the applications of the ideas developed in this work.

Chapter 3 presents the variational Monte Carlo (VMC) method in order to compute the universal equation of state, the method is based on the minimization of the variance of energy, as opposed to the energy itself in standard methods. The theory illustrates how the equations of state can be computed exactly, and the existence and the importance of long-range atom-atom correlation under strong confinement.

The ideas developed in Chapter 3 are tested, in Chapter 4, against some known

results, such as few and many hard spheres in a symmetric harmonic trap. Explicit numerical results are presented for few atoms in a trap and many atoms as a homogeneous system.

The results presented in Chapter 4 are used to provide a quantitative understanding of the shape-dependent confinement correction that is important for few atoms under strong confinement. The physical significance of the results is also discussed. There is also a brief discussion of a future direction which the current work could easily lead into.

# Chapter 2

## Background

### 2.1 Many-Body systems

Since the time of the ancient civilisations, philosophers have pondered the mysteries of the universe. One of the problems under investigation is the interactions between the various bodies which are observed in our environment. It eventually became clear that the universe could be modelled as a system of interacting bodies.

Many body systems cover a wide range of subjects, energies and length scales in science. From the behaviour of stars and galaxies to the nature of subatomic particles, many body systems have played a core part in the understanding and exploration of our environment. Subjects such as Physics, Chemistry and Biology have all sought to understand the behaviour of many body systems. In many cases success has been limited due to our simplistic understanding of interacting bodies. Classically Newtons laws of motion allowed one to predict the behaviour of simple systems. Any complicated objects are modelled as point particles or a centre of mass

is introduced in order to simplify the problem at hand. Newton's theory of Gravitation enjoyed much success in describing the motion of celestial objects, however, any set of objects which could not be simplified to a system of particles could not be accurately modelled by Newton's laws. Newton's theory also struggled to describe phenomena of electromagnetism, wave behaviour and the microscopic behaviour of matter. These difficulties motivated the likes of Faraday, Maxwell, Boltzmann and others to seek new methods and descriptions to investigate matter and energy.

### 2.1.1 Statistical Physics

One of the most important methods used to investigate matter and energy are the tools of statistics and probability. The use of statistical methods in Physics allowed scientists to study macroscopic properties of matter, these tools became an invaluable resource when investigating the thermodynamics of a system; the field of thermodynamics is one that studies the macroscopic behaviour of a system by drawing conclusions directly from experiments. In thermodynamics a *thermodynamic state* is one which is completely described by a set of parameters, such as pressure (P), volume (V), temperature (T) etc, if the system did not change with time then one would assume that the state is in *thermodynamic equilibrium*. Thermodynamic equilibrium is described by an *equation of state* which is a functional relationship between the parameters of the system, it may take the form [7]

$$f(P, V, T) = 0, \tag{2.1}$$

$f$  is a representation of the physical system being described. An example of the equation of state is Boyle's law which describes the ideal gas. The ideal gas is an idealised situation which describes a dilute non-interacting gas, experimentally all gases have universal behaviour which approximates an ideal gas. The parameters of an ideal gas are P, V and T

$$PV = Nk_B T, \quad (2.2)$$

where N would be the number of gas particles and  $k_B$  is Boltzmann's constant ( $k_B = 1.38 \times 10^{-23} J/K$ ), this equation describes the universal character of an ideal gas. The ideal gas is a simple approximation of a *real* dilute gas, therefore, it has significant limitations in that it assumes the particles are non-interacting; real gases are always interacting via some interaction potential. Van der Waals, inspired by Boltzmann, produced a simple qualitative way to improve the equation of state, of a dilute gas, by incorporating the effects of molecular interaction. The result is the Van der Waals equation of state [7],

$$(V - b)\left(P - \frac{a}{V^2}\right) = N_A k_B T, \quad (2.3)$$

where  $a$  and  $b$  are constant characteristics of the system and  $N_A$  is Avogadro's number ( $N_A = 6.023 \times 10^{23} \text{ particles/mol}$ ).

Van der Waal realised that the real interaction potential, Figure 2-1, could be replaced with a hard wall and a tail, such as Figure 2-2.

This is an improvement upon Boyle's law in that it established a relationship

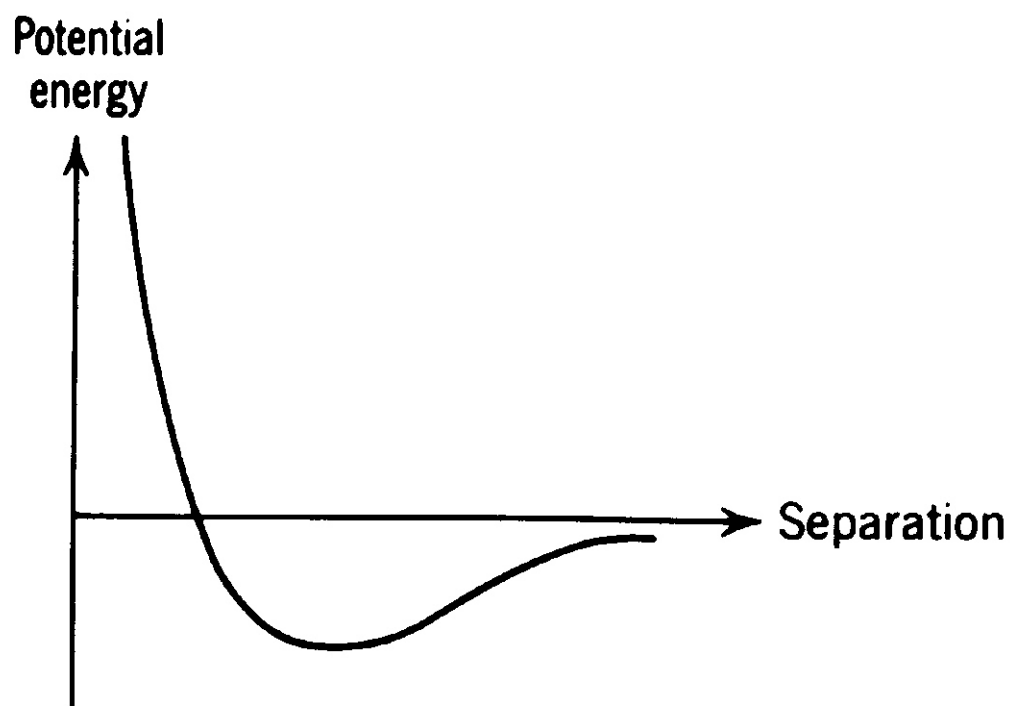


Figure 2-1: An example of the real interaction potential between atoms.

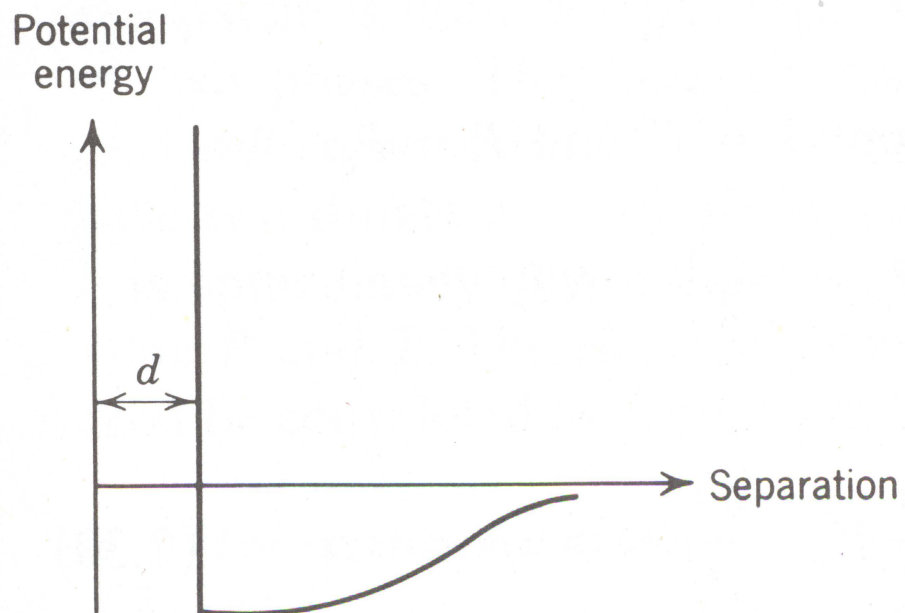


Figure 2-2: Van der Waals potential.

between the microscopic and the macroscopic properties of a gas. It was soon self-evident that a clear picture of the macroscopic behaviour of matter involved a clear understanding of the microscopic behaviour of matter. Although there were ideas regarding the nature of matter, it was not until a Quantum mechanical picture of nature started to present itself that scientists were able to understand the microscopic.

### 2.1.2 Quantum Mechanics

The formulation of Quantum Mechanics brought about a plethora of new states and properties of matter which were to be discovered and investigated. Quantum theory was born when particle concepts were introduced into the wave theory of light by Planck, who introduced the quantum  $h$ . At the heart of Quantum theory are the statistical methods which are used to formulate a description of nature based on the wave-particle duality of light and matter. The statistical methods involve formulating a Hamiltonian operator of the system, known as Schrödinger's equation,

$$\widehat{H} = -\frac{\hbar^2}{2} \sum_{i=1}^N \left( \frac{\nabla_i^2}{m_i} + V_{ext}(\mathbf{r}_i) \right) + \sum_{i<j=1}^N v(r_{ij}) . \quad (2.4)$$

with  $V_{ext}(\mathbf{r})$  is the external *trapping* potential and  $v(r_{ij})$  describes the interactions between the individual particles. The Schrödinger equation may be derived from de Broglie's principle [8]. The time-independent solutions of the Schrödinger equation, known as stationary states, describe the *state* of the system. This solution is known as the wavefunction,  $\Psi(\mathbf{R})$ , which is a function of the particle positions, the shape of the interaction potential and the external potential determine the form of the

wavefunction. The wavefunction is related to the probability of the system,

$$P = \int d\tau \Psi^* \Psi, \quad (2.5)$$

where  $d\tau$  is a volume element, the average energy is then expressed as,

$$E = \frac{\int d\tau \Psi^* \widehat{H} \Psi}{\int d\tau \Psi^* \Psi} = \frac{\langle \Psi | H | \Psi \rangle}{\langle \Psi | \Psi \rangle}. \quad (2.6)$$

Therefore, in order to develop a complete understanding of a quantum system one must have a complete understanding of the wavefunction,  $\Psi(\mathbf{R})$ . In regards to many-body systems, the specific shape of the wavefunction is highly dependent on the interactions between each particle. The interactions between atoms can be highly complex and are dependent on the structure of the atom, in order to include this complexity in the wavefunction one must be able to describe the interactions in an adequate way and also be able to formulate them into Eq. (2.4) in order to solve for the wavefunction. One of the major stumbling blocks in the past has been how to adequately treat many atom systems, especially since the interactions between the atoms play a significant role.

### 2.1.3 Many-Atom Interactions

Matter is capable of displaying many properties and each *state* of matter exhibits different types of behaviour. This behaviour, for the most part, is governed by the interactions between individual atoms. Particles are capable of many types of interactions, some of these interactions are long-range or short-range in nature. Many

complicated interactions can be presented as one or more simple interactions. A typical interaction one may come across is the Coulomb interaction between two point charges,

$$v(r_{ij}) = \kappa \frac{q_i q_j}{r_{ij}}, \quad (2.7)$$

where  $v(r)$  represents the form of the potential energy of the system,  $q_1$  and  $q_2$  are the respective charges,  $r_{12}$  is the interparticle distance and  $\kappa$  is a constant. This form of interaction is used in the Schrödinger's equation, Eq. (2.4) to derive the eigenstates of the hydrogen atom, examples of which may be found in literature [8, 9, 10]. Although the coulomb interaction is suitable for the Hydrogen atom, it is inadequate to describe the interactions between multi-electron atoms. Most of our existing understanding is based on the shape-independent approximation for the atomic interaction which is derived from the old theory for slow atomic scattering known as the effective range expansion. The effective range expansion concludes that the shape of the potential is not important as long as it provides the correct scattering length. The results are relatively simple and universal, but have a limited range of applicability, overcoming these limitations requires a better description of the atomic interaction.

In general a many-atom system involves the atoms interacting with each other in a whole host of ways. The interaction is usually expressed as a sum of series,

$$\Phi(r) = \sum_{ij} \Phi_{ij}(r) + \sum_{ijk} \Phi_{ijk}(r) + \sum_{ijkl} \Phi_{ijkl}(r) + \dots \quad (2.8)$$

where  $ij$  refers to atom pairs,  $ijk$  refers to all atom triplets, etc. However, the

majority of interactions may be reduced to a pair potential,

$$\Phi(r) = \sum_{ij} \Phi_{ij}(r) . \quad (2.9)$$

A diffuse atomic state has both short and long range interactions. The short range interaction only plays a role in determining the scattering length, while the long range interaction determines the universal behaviour. All atoms see the same type of long-range interactions,  $v(r) = -C_n/r^n$ , and each long-range interaction has a length scale associated with it,

$$\beta_n = \left( \frac{mC_n}{\hbar^2} \right)^{\frac{1}{n-2}} . \quad (2.10)$$

The long range atomic interaction may be expressed as

$$v(r) \longrightarrow -\frac{C_6}{r^6} - \frac{C_8}{r^8} - \dots , \quad (2.11)$$

in which  $\beta_6$  is the longest length scale and is 60 - 200 au for alkali metals. One may design an effective potential,  $V_{eff}$ , which eliminates all the length scales shorter than  $\beta_6$  and still has the correct form of the long range interaction. One example is,

$$V_{eff}(r) = \begin{cases} \infty & , \quad r \leq r_0 \\ -\frac{C_6}{r^6} & , \quad r > r_0 \end{cases} , \quad (2.12)$$

as referenced in [11, 12]. In order to incorporate this into a many-body system one may use an effective Hamiltonian such as,

$$H_{\beta_6} = \sum_{i=1}^N \frac{\hbar^2}{2m} \nabla_i^2 - \sum_{i<j} v_{eff}(r_{ij}). \quad (2.13)$$

This allows one to determine the universal equation of state, which for a homogeneous system would then be,

$$E_s/N = \Omega^{(6)}(\rho_s, a_{0s}). \quad (2.14)$$

The Physics of many-atom systems has focused on three aspects [10],

1. Ground state properties
2. Excited states
3. Temperature dependent phenomena

This dissertation is focused on the first two, hence all the ideas developed in this work are for zero temperature physics.

The problem of understanding the properties of quantum many-particle systems possessing large degrees of freedom permeates all of theoretical physics. Therefore the mathematical methods developed over the centuries comprise an important aspect of understanding many-body physics.

#### 2.1.4 Tools for Investigating Many-Atom Systems

When investigating few and many body systems the important step is to acquire the equation of state; which is the energy per particle as a function of density. Once

this is obtained one may have a good understanding of the system at hand. The mean field result,

$$E/N = \frac{2\pi^2 a_0}{m} \rho, \quad (2.15)$$

applies to a quantum gas of hard spheres, this may be improved upon when perturbation theory is considered,

$$E/N = \frac{2\pi^2 a_0}{m} \rho \left[ 1 + \frac{128}{15} \sqrt{\frac{\rho a_0^3}{\pi}} \right], \quad (2.16)$$

where  $a_0$  is the s-wave scattering length and  $\rho$  is the number density of the system. This equation is known as the LHY equation [13, 14] and can be applied to a Bose gas where all the particles interact via a repulsive hard sphere interaction. Although both these equations represent the universal properties of Bose systems, their range of applicability is limited. They work well when  $\rho a^3 \ll 1$  and  $\rho \beta_6^3 \ll 1$ , but fail to make any good predictions outside this range. Other work done in this field has been the Diffusion Monte Carlo (DMC) study of liquid Helium. The DMC method worked very well for liquid Helium because liquid Helium was the true ground state of that particular system; however, when investigating the excited state of an atomic system the DMC method would not perform very well. This is due to the fact that the DMC method is not able to *sample* a wavefunction which is not positive everywhere. Obviously this leads to major difficulties when dealing with excited states of atomic systems and even the ground state of a fermionic system. However, this does not

apply to all Monte Carlo methods, the variational Monte Carlo (VMC) method is one which may be used to investigate the excited states of an atomic system as well as the ground state.

## 2.2 Monte Carlo Methods

Monte Carlo methods have played an important role in our understanding of a variety of quantum systems, especially few- and many-body quantum systems with strong interactions that are difficult to treat otherwise (see, e.g., Refs. [15, 16, 2, 1, 17]). It is also well-known, however, that most quantum Monte Carlo methods [16] are formulated in such a way that they are strictly applicable only to the ground state of a quantum system, a restriction that has severely limited their applicability. Consider, for example, the gaseous Bose-Einstein condensates (BEC) of alkali-metal atoms (see, e.g., [18]). Any theory that intends to treat the real atomic interaction has to deal with the fact that the gaseous BEC branch of states are in fact highly excited states of a many-atom system. There are many branches of states of lower energies, including the first branch of liquid states as suggested and studied recently [19].

### 2.2.1 Variational Monte Carlo

The relative merits of different Monte Carlo methods are well documented [16]. The choice here of the variational Monte Carlo method (VMC) is for a number of reasons:

1. VMC always works, for bosons, fermions, or excited states, provided one picks the right trial wave function.
2. VMC provides the most transparent understanding of many-body wave function, and is thus the best for conceptual purposes.
3. The advantages of other Monte Carlo methods [16], such that being a “black box”, mostly disappear when applied to fermions or to the excited states of a many-body system.
4. The result of VMC can always be used as the starting point upon which further adjustment or relaxation of the wave function can be allowed, if at all necessary. More specifically, it can be used to fix the nodal structure and provide importance sampling [15].

The difficulty, or the challenge of VMC, is in choosing a proper trial wave function. Otherwise no converged result would be obtained, as reflected in the fact that the variance of energy would be of the same order of, or greater than, the average value being evaluated. The same challenge can, however, also be regarded as an opportunity, as it forces one to understand the wave function.

The variational method in the form of an algorithm:

1. A many-body wave function is constructed  $\Psi_\alpha(\mathbf{R})$  which depends on a set of variational parameters and the coordinates of all the particles,  $\mathbf{R} = \mathbf{r}_1, \dots, \mathbf{r}_N$ .

2. The expectation value of the energy is computed

$$\langle E \rangle = \frac{\langle \Psi_\alpha | H | \Psi_\alpha \rangle}{\langle \Psi_\alpha | \Psi_\alpha \rangle} \quad (2.17)$$

3. Vary  $\alpha$  according to some minimisation algorithm and return to step 1.

The loop is completed when the minimum energy has been reached according to some criterion. In most many-body problems the wave function may hold very small values in large parts of configuration space, therefore it is inefficient to place walkers in homogeneously random fashion. A Metropolis algorithm is used in which the walkers are *encouraged* to sample region of space where the wavefunction takes on large values. If we choose a trial wavefunction for our system,  $\Psi_T$ , then we may define,

$$E_{Loc} = \frac{\widehat{H}\Psi_T}{\Psi_T}, \quad (2.18)$$

where  $E_{Loc}$  is referred to as the *local energy*, and  $\widehat{H}$  is the hamiltonian of the system. As Eq (2.18) implies, the closer  $\Psi_T$  approaches the exact wavefunction the smaller the variations in  $E_{Loc}$  with position, if  $\Psi_T$  is an exact eigenfunction of of the Hamiltonian then  $E_{Loc}$  becomes constant. The expectation value of the energy Eq (2.17) may now be expressed as,

$$\langle E \rangle = \frac{\int d\tau \Psi_T^* \Psi_T E_{Loc}}{\int d\tau \Psi_T^* \Psi_T} \geq E_0, \quad (2.19)$$

where  $E_0$  is the true ground state energy. Using this formulation one may investigate the ground state of an atomic system. One of the more interesting systems is the Bose-Einstein condensate (BEC), this system involves all the particles condensing into a single state. Particles which are capable of displaying this behaviour are known as *bosons*; bosons are particles which have a whole integer spin angular momentum number. Although all bosons are capable of forming a BEC below a critical temperature, not all BECs are the true ground states of that particular system.

## 2.3 Quantum Defect Theory

Another important tool of atomic and molecular physics is Quantum defect theory which became significant in combining spectroscopy with collision theory.

Quantum defect theory has its origins in Rydberg's original 1890 paper, [20], with the equation,

$$E_n = -\frac{R_\lambda}{(n - \delta_l)^2}, \quad (2.20)$$

where  $R_\lambda$  is the Rydberg constant and  $\delta_l$  is the quantum defect dependent on the angular momentum  $l$  of an excited electron in a hydrogen-like atom. This equation represents an example of universal property as it allows one to obtain a universal spectrum with long-range Coulomb interaction,  $(-Z/r)$ . The origins of the defect are the ionic core of the remaining electrons, each electron experiences this distribution to different degrees. Electrons with a small  $l$ -value are able to penetrate into the core which makes  $\delta_l$  small for  $l > 3$ . In order to understand the physical nature of

the quantum defect one may consider the motion of an electron in an multi-electron atom. The electron is subject to the long-range Coulomb field (due to the core) and the short-range multiparticle interactions. Each interaction has its own energy and length scale. The quantum defect has its roots in the short-range interactions, which do not cause drastic changes in energy. As a result of this the quantum defect is, to a first-order approximation, constant from one energy level to the next at the higher levels.

For quantum systems with  $-C_n/r^n$  types of long-range interaction one may obtain a universal spectrum for each  $n$  using a two-body quantum defect theory, each  $n$  would also have universal scattering properties. Potentials with the same short-range parameter, such as scattering length, have the same bound spectra, the same scattering properties and the same wavefunctions over a wide range of energies around the threshold. As discussed in section( 2.1.3) universal properties exist at length scale  $\beta_6$  and are determined by the long range interaction. A single short-range parameter,  $K^c$ , is chosen to describe all the states around the threshold regardless of the type of state or its angular momentum.  $K^c$  is a short range parameter which best describes the short-range atomic interaction which may differ from  $-C_6/r^6$ . Both the energy and the angular momentum dependencies around the dissociation limit are dominated by the long-range interaction.

Present day quantum defect theory has evolved into an elaborate idea known as *multichannel quantum-defect theory* (MQDT), which is widely applied in atomic physics.

## 2.4 Bose-Einstein Condensation

### 2.4.1 Historical

In 1924 Satyendra Nath Bose, and Albert Einstein in 1925, predicted that below a critical temperature,  $T_c$ , all the particles in a system undergo a phase change and occupy the lowest energy quantum state, [21, 22], particles which follow this behaviour are known as *Bosons*. All particles may be divided into one of two classes; Bosons or Fermions. Bosons are particles in which the spin angular momentum is a whole integer, and the wavefunction for a system of identical Bosons is symmetric under interchange of any two particles. On the other hand particles which are classed as Fermions have a half-odd-integer spin and an antisymmetric wavefunction.

This phase change allows quantum effects to be observed on the macroscopic scale, particles which undergo this phase change are known as Bose-Einstein condensates (BEC). A BEC is a phase-transition, which does not depend on the specific interactions between particles. It is based on the indistinguishability and the wave nature of particles, both of which are at the heart of quantum mechanics.

The diagram, figure 2-3 shows the stages in creating a BEC. Initially atoms at high temperatures have a negligible thermal wavelength,  $\lambda_{dB}$ , which is much smaller than the interparticle spacing,  $d$ . The thermal wavelength is expressed as,

$$\lambda_{dB} = \sqrt{\frac{2\pi\hbar^2}{mk_B T}}. \quad (2.21)$$

At these high temperatures,  $T \gg T_c$ , particles may be treated as weakly interacting

billiard balls, figure 2-3. If the temperature of the system is reduced then the thermal wavelength starts to increase in size and become significant, it is at this stage quantum effects start to become important as the particles are no longer point-like billiard balls but are actually *wave – packets*, Figure 2-3. At the critical temperature we have a BEC and the thermal wavelength becomes similar in size to the interparticle distance,  $\lambda_{dB} \approx d$ . At this point the individual wavefunctions start to overlap, a fraction of the bosons are in a BEC state whereas the remainder are in an excited state. If the temperature is reduced even further to  $T = 0$  the system reduces to a pure Bose condensate where all the particles are in the same state.

### 2.4.2 Previous BECs

Typically one may create a BEC by cooling a substance below its critical temperature,  $T_c$ . Historically the first BECs under investigation were the superconducting metals, where two electrons of opposite spin combine to form a boson (also known as a Cooper pair). A qualitative understanding of superconductors may be obtained by treating the electron pairs as a BEC. Aside from superconductors one may also create a liquid BEC by cooling Helium below its critical temperature. The Helium liquids,  $^4\text{He}$  and  $^3\text{He}$ , do not condense into solids at very low temperatures. The low mass of the Helium atom makes the zero point energy large enough to overcome solidification. Below the critical temperature liquid Helium is a superfluid with many unique properties. Two of the most important properties of superfluid He are the ability to flow without friction and the existence of quantized vortices within the fluid.

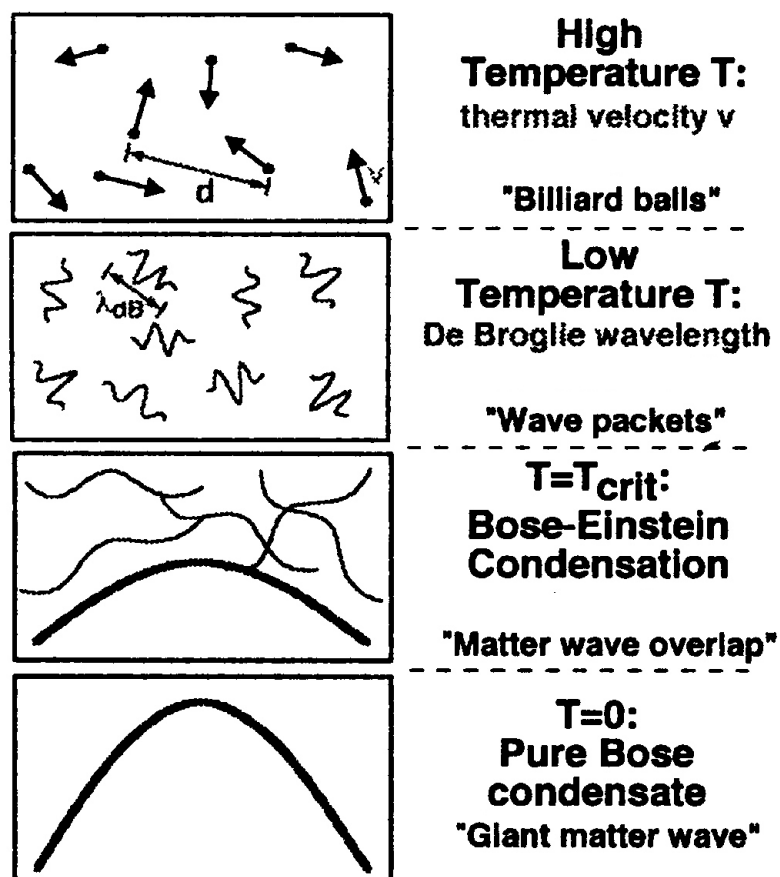


Figure 2-3: The behaviour of particles above and below  $T_c$ .

## 2.5 Dilute Bose Gases

### 2.5.1 Cooling

Although liquid BECs were produced in a laboratory many decades ago, the gaseous state was only produced in 1995 using the powerful laser cooling methods developed in recent years. Dilute gaseous BECs are created via a combination of laser cooling and evaporative cooling. Since the speed of particles is directly proportional to the the temperature of a system of particles, one may cool a substance by reducing the motion of the individual particles.

In the initial experiments to create a gaseous BEC [23], laser cooling was used to reduce the temperature of Rubidium atoms from room temperature to  $1\mu K$ . The gas was then trapped magnetically and further cooled to approximately  $1nK$  by evaporative cooling. Figure 2-4 represents a simple illustration as to how atoms may be cooled using evaporative cooling.

When a gas of bosonic particles is cooled below a critical temperature,  $T_c$ , it condenses into a BEC. The condensate consists of a macroscopic number of particles, which are all in the ground state of the system. For a uniform gas of free particles one may estimate the transition temperature to be [24],

$$T_c = C \frac{\hbar^2 \rho^{2/3}}{mk_B} \quad (2.22)$$

where  $C \approx 3.3$ .

Figure 2-5 is a false color image of the velocity distribution of a gas of Rubidium

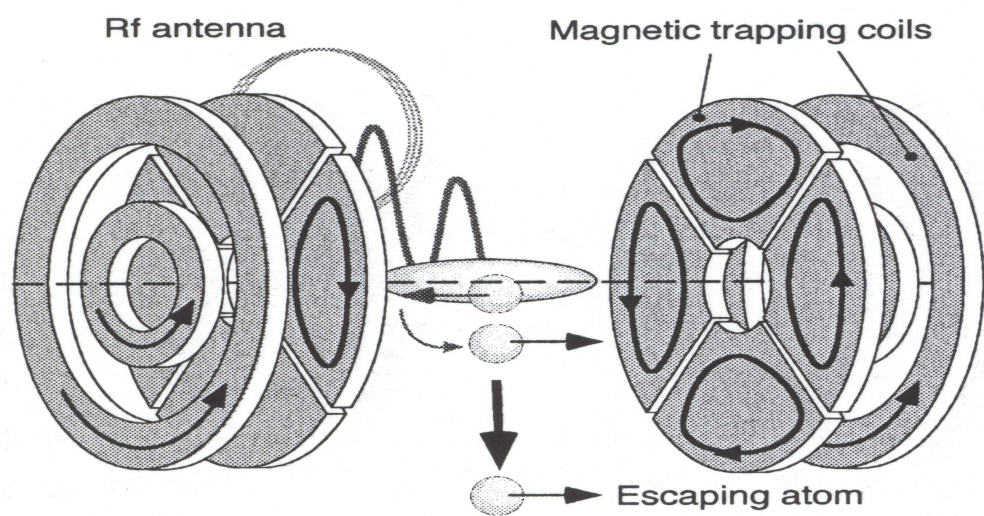


Figure 2-4: Experimental setup.

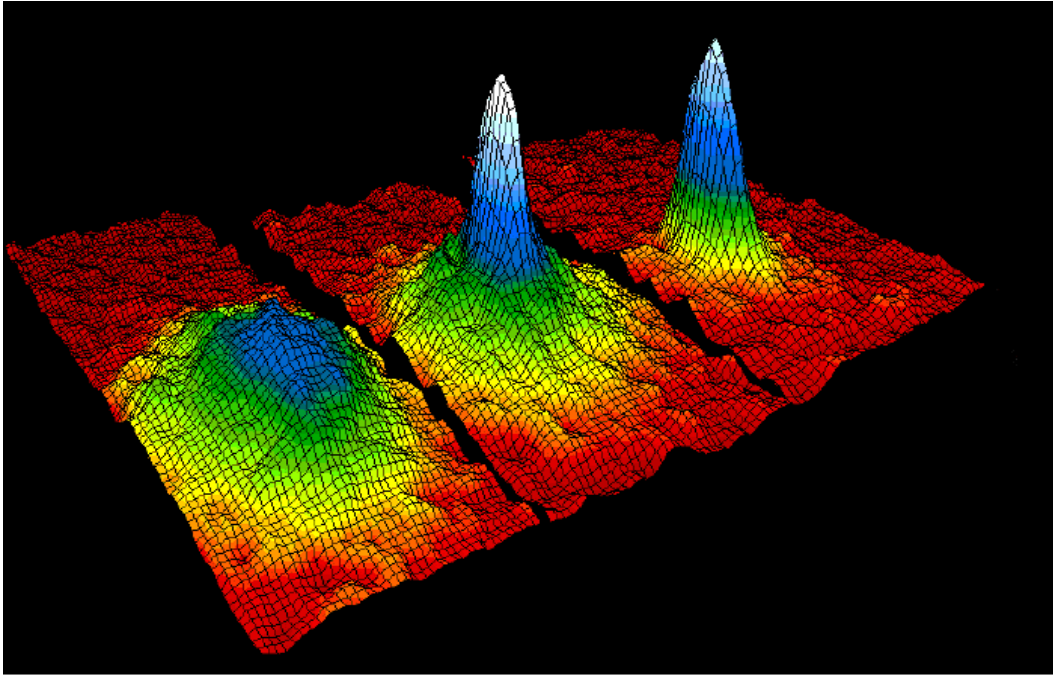


Figure 2-5: Left: Just before the BEC. Centre: Just after the appearance of the condensate. Right: After further evaporation - nearly a pure condensate.

atoms which confirmed the discovery of a new phase of matter. The figure represents the number of atoms at a particular velocity, where red represents the fewest atoms and white represents the greatest number of atoms.

At present gaseous BECs have been created using group I elements, Rubidium, Sodium, Lithium and Hydrogen. Much of the appeal of atomic clouds is based on the fact that they are dilute in the sense that their scattering length is much less than the interparticle spacing. Although group I elements have one outer electron, which suggests they may be Fermions, they are in fact Bosons due to an interaction between the nuclear and electronic spin degree of freedom.

# Chapter 3

## Many Atom Quantum Theory

### 3.1 Variational Method

In Quantum theory one typically uses the solutions of the Schrödinger equation to describe the physical system at hand. In a few situations it is possible to find an analytical solution to the Schrödinger equation; however in most cases one is required to perform an integration in order to calculate the expectation values. The integration itself is usually done numerically which requires a huge amount of computer time and memory. The variational method allows one to find a solution to the Schrödinger equation by restricting the solutions to a subspace of Hilbert space. By restricting the solutions one is able to compute the expectation values of the system in a more efficient manner. If we desire to calculate the expectation value of the energy then we may use the functional,

$$E[\Psi] = \frac{\int d\tau \Psi^*(\tau) H \Psi(\tau)}{\int d\tau \Psi^*(\tau) \Psi(\tau)} = \frac{\langle \Psi | H | \Psi \rangle}{\langle \Psi | \Psi \rangle}. \quad (3.1)$$

The stationary states are then defined by stating that a small change in the wavefunction,  $\delta\Psi$ , produces a change in  $E$  which vanishes to the first order,

$$\delta E = \frac{\langle \Psi + \delta\Psi | H | \Psi + \delta\Psi \rangle}{\langle \Psi + \delta\Psi | \Psi + \delta\Psi \rangle} - \frac{\langle \Psi | H | \Psi \rangle}{\langle \Psi | \Psi \rangle} = 0, \quad (3.2)$$

this should disappear for small changes in  $\Psi$ , therefore

$$H\Psi = E\Psi. \quad (3.3)$$

It is this very idea which is the basis of the variational Monte Carlo (VMC) method.

## 3.2 Variational Monte Carlo

### 3.2.1 Local Energy

In order to calculate the expectation value of the energy one must derive an explicit form the local energy,  $E_{Loc}$ , as described in section (2.2.1), which one encounters in the standard VMC.

Consider an  $N$ -atom Bose system described by the Hamiltonian

$$\widehat{H} = \sum_{i=1}^N \hat{h}_i + \sum_{i<j=1}^N v(r_{ij}), \quad (3.4)$$

with

$$\hat{h}_i = -\frac{\hbar^2}{2m}\nabla_i^2 + V_{ext}(\mathbf{r}_i), \quad (3.5)$$

where  $V_{ext}$  describes the external “trapping” potential, and  $v(r)$  represents the interaction between atoms that has a behavior of  $v(r) \rightarrow -C_6/r^6$  in the limit of large  $r$ .

Such an  $N$ -atom Bose system has of course many different states. We focus ourselves here on the lowest gaseous Bose-Einstein condensate (BEC) state, which can be defined as the state that evolves from the lowest  $N$ -free-particle state in a trap as one turns on an atomic interaction with positive scattering length. For this particular state, we take the variational trial wave function to be of Jastrow form [25]

$$\Psi = \left[ \prod_{i=1}^N \phi(\mathbf{r}_i) \right] \prod_{i<j=1}^N F(r_{ij}). \quad (3.6)$$

This is a product of single particle terms  $\phi(r)$  and a product of correlation terms  $F(r)$ . It is straightforward to show that the expectation value of energy for such a state can be written as

$$\begin{aligned} E &= \frac{\int d\tau \Psi^* H \Psi}{\int d\tau \Psi^* \Psi} \\ &= \frac{\int d\tau \Psi^* \Psi E_{Loc}}{\int d\tau \Psi^* \Psi}, \end{aligned} \quad (3.7)$$

where the integrations are over all  $N$ -atom coordinates,  $E_{Loc}$  is the local energy and is defined as,

$$E_{Loc} = \frac{\widehat{H}\Psi}{\Psi}. \quad (3.8)$$

For identical particles Eq. 3.7 now becomes

$$E = \frac{\int d\tau \Psi^* \Psi \frac{1}{\Psi} \left( N\hat{h}_1 + \sum_{i<j=1}^N v(r_{ij}) \right) \Psi}{\int d\tau \Psi^* \Psi}, \quad (3.9)$$

which makes  $E_L$ ,

$$E_{Loc} = N \left( -\frac{\hbar^2}{2m} \right) \frac{1}{\Psi} \nabla_1^2 \Psi + NV_{ext}(\mathbf{r}_1) + \sum_{i<j=1}^N v(r_{ij}). \quad (3.10)$$

Since the wavefunction is of the form Eq. (3.6), the local energy can be written as the sum of three terms whose contributions to the energy depend on the 1-body, 2-body, and three-body correlation functions, respectively:

$$E_{Loc} = E_L^{(1)}(\mathbf{r}_1) + E_L^{(2)}(\mathbf{r}_1, \mathbf{r}_2) + E_L^{(3)}(\mathbf{r}_1, \mathbf{r}_2, \mathbf{r}_3). \quad (3.11)$$

Here

$$E_L^{(1)} = \frac{1}{\phi(\mathbf{r}_1)} \left[ -\frac{\hbar^2}{2m} \nabla_1^2 \phi(\mathbf{r}_1) \right] + V_{ext}(\mathbf{r}_1), \quad (3.12)$$

$$E_L^{(2)} = E_{L1}^{(2)} + E_{L2}^{(2)}, \quad (3.13)$$

with

$$E_{L1}^{(2)} = (N-1) \frac{1}{2} \left\{ \frac{1}{F(r_{12})} \left[ -\frac{\hbar^2}{m} \nabla_1^2 F(r_{12}) \right] + v(r_{12}) \right\}, \quad (3.14)$$

$$E_{L2}^{(2)} = -(N-1) \left( \frac{\hbar^2}{m} \right) \frac{1}{\phi(\mathbf{r}_1) F(r_{12})} [\nabla_1 \phi(\mathbf{r}_1)] \cdot [\nabla_1 F(r_{12})], \quad (3.15)$$

and

$$E_L^{(3)} = -\frac{1}{2}(N-1)(N-2) \left( \frac{\hbar^2}{m} \right) \times \frac{1}{F(r_{12})F(r_{13})} [\nabla_1 F(r_{12})] \cdot [\nabla_1 F(r_{13})] . \quad (3.16)$$

Once  $\phi$  and  $F$  are chosen, Eq. (3.7) can be evaluated using Metropolis Monte Carlo method (see, e.g., [26]), and the variational parameters are then varied to find the stationary energies.

### 3.2.2 Trial Wavefunction

The success, or the failure, of a VMC calculation depends exclusively on the proper choice of the wave function, for this work the trial wavefunction is chosen to be of the form Eq. (3.6). The choice of  $\phi$  is fairly standard and is based on the independent-particle solution in the external potential. The choice of  $F$  is less obvious, and depends on the understanding of atom-atom correlation in a trap. Our choice of  $F$  is based the following physical considerations. (a) Atom-atom correlation at short distances is determined by two-body interaction. (b) Atoms in a trap can have long-range correlation that becomes important under strong confinement, as suggested by our recent work on two atoms in a trap [27]. Specifically, we choose our  $F$  as

$$F(r) = \begin{cases} Au_\lambda(r)/r & , \quad r < d \\ (r/d)^\gamma & , \quad r \geq d \end{cases} . \quad (3.17)$$

Here  $u(r)$  satisfies the Schrödinger equation:

$$\left[ -\frac{\hbar^2}{m} \frac{d^2}{dr^2} + v(r) - \lambda \right] u_\lambda(r) = 0 , \quad (3.18)$$

for  $r < d$ .  $\gamma$  is the parameter characterizing the long-range correlation between atoms in a trap, with  $\gamma = 0$  (meaning  $F = 1$  for  $r > d$ ) corresponding to no long-range correlation. Both  $d$  and  $\gamma$  are taken to be variational parameters, in addition to the variational parameters associated with the description of  $\phi$ . The parameters  $A$  and  $\lambda$  are not independent and are determined by matching  $F$  and its derivative at  $d$ .

The key difference between our choice of  $F$  and the standard choices [17], in addition to the systematic treatment of atomic interaction to be discussed in the next section, is the allowance for the long-range correlation characterized by parameter  $\gamma$  [27]. One can easily verify that regardless of the model potential used for  $v$  (such as the hard sphere potential), a choice of  $F$  without long-range correlation, such as [17]

$$F(r) = 1 - a_0/r , \quad (3.19)$$

would not have led to converged VMC results under strong confinement. This explains why the existing Monte Carlo results for few atoms under strong confinement have come from diffusion Monte Carlo (DMC) [1], but not from VMC, which was successful for weak confinements [17].

### 3.2.3 Variance Minimisation

Existing quantum Monte Carlo methods are mostly based on the fact that for an arbitrary trial wave function satisfying proper boundary conditions, we have

$$E_T[\Psi_T] \equiv \frac{\langle \Psi_T | \widehat{H} | \Psi_T \rangle}{\langle \Psi_T | \Psi_T \rangle} \geq E_0 , \quad (3.20)$$

which means that the ground state wave function is the one that minimizes the energy functional  $E_T[\Psi_T]$ . The proof can be found in standard quantum mechanics textbooks (see, e.g., [28, 29]).

The variance minimization variational Monte Carlo method (VMVMC), as proposed here, is based on the functional

$$\eta[\Psi_T] \equiv \frac{\langle \Psi_T | \widehat{H}^2 | \Psi_T \rangle}{\langle \Psi_T | \Psi_T \rangle} - \left[ \frac{\langle \Psi_T | \widehat{H} | \Psi_T \rangle}{\langle \Psi_T | \Psi_T \rangle} \right]^2 \geq 0 . \quad (3.21)$$

The proof of Eq. (3.21) and its physical meaning can be best understood by expanding the trial wave function using the complete basis defined by

$$\widehat{H} |\Psi\rangle = E_n |\Psi\rangle \quad (3.22)$$

to write  $\eta[\Psi_T]$  as

$$\eta[\Psi_T] = \frac{\sum_m |\langle \Psi_m | \Psi_T \rangle|^2 (E_m - E_T)^2}{\sum_m |\langle \Psi_m | \Psi_T \rangle|^2} . \quad (3.23)$$

From Eq. (3.23), it is clear that zero is the minimum of the functional  $\eta[\Psi_T]$ , and this minimum is reached when and only when  $E_T = E_n$  and  $\langle \Psi_m | \Psi_T \rangle = 0$  for  $m \neq n$ ,

namely, only when  $|\Psi_T\rangle$  is an eigenstate of energy as defined by Eq. (3.22). This statement is equally applicable to the ground and the excited states of a quantum system.

The implementation of VMVMC, based on the minimization of the variance of energy  $\eta[\Psi_T]$ , is straightforward. It does not require much more than the standard VMC.

Consider  $N$  identical particles in an external potential and interacting via pairwise interactions. It is described by a Hamiltonian:

$$\widehat{H} = \sum_{i=1}^N \widehat{h}_i + \sum_{i<j=1}^N v(r_{ij}) , \quad (3.24)$$

with

$$\widehat{h}_i = -\frac{\hbar^2}{2m} \nabla_i^2 + V_{ext}(\mathbf{r}_i) . \quad (3.25)$$

Here  $V_{ext}(\mathbf{r})$  is the external “trapping” potential, and  $v(r)$  is the interaction between particles.

For the evaluation of the energy functional, we have

$$\begin{aligned} \langle \Psi_T | \widehat{H} | \Psi_T \rangle &= \langle \Psi_T | N \widehat{h}_1 + \frac{1}{2} N(N-1) v_{12} | \Psi_T \rangle \\ &= \int d\tau \Psi_T^* \Psi_T \frac{1}{\Psi_T} \{ N \widehat{h}_1 + \frac{1}{2} N(N-1) v(r_{12}) \} \Psi_T \\ &= \int d\tau \Psi_T^* \Psi_T E_{Loc}(\tau) , \end{aligned} \quad (3.26)$$

where  $\tau$  represents an  $N$  particle configuration specified by their  $3N$  coordinates.

$E_{Loc}$  is the so-called local energy, and is given by

$$E_{Loc} = N \left( -\frac{\hbar^2}{2m} \right) \frac{1}{\Psi_T} \nabla_1^2 \Psi_T + N V_{ext}(\mathbf{r}_1) + \frac{1}{2} N(N-1) v(r_{12}) . \quad (3.27)$$

The average energy is therefore

$$E_T = \frac{\int d\tau \Psi_T^* \Psi_T E_{Loc}(\tau)}{\int d\tau \Psi_T^* \Psi_T} . \quad (3.28)$$

This is the standard integral in VMC, and can be evaluated using standard Monte Carlo methods such the Metropolis method (see, e.g., [26]).

In order to calculate the variance of energy, one must also determine the average of  $\widehat{H}^2$ . This can be done by first noting that, similar to Eq. (3.26), we have

$$\langle \Psi_m | \widehat{H} | \Psi_T \rangle = \int d\tau \Psi_m^* \Psi_T E_{Loc}(\tau) , \quad (3.29)$$

where  $|\Psi_m\rangle$  is an eigenstate of energy as defined by Eq. (3.22). We have therefore

$$\begin{aligned} \langle \Psi_T | \widehat{H}^2 | \Psi_T \rangle &= \sum_m \langle \Psi_T | \widehat{H} | \Psi_m \rangle \langle \Psi_m | \widehat{H} | \Psi_T \rangle \\ &= \sum_m \langle \Psi_m | \widehat{H} | \Psi_T \rangle^* \langle \Psi_m | \widehat{H} | \Psi_T \rangle \\ &= \sum_m \int d\tau d\tau' [\Psi_m(\tau') \Psi_T^*(\tau') E_{Loc}^*(\tau') \\ &\quad \times \Psi_m^*(\tau) \Psi_T(\tau) E_{Loc}(\tau)] . \end{aligned} \quad (3.30)$$

Using the completeness relation

$$\sum_m \Psi_m(\tau') \Psi_m^*(\tau) = \delta(\tau' - \tau), \quad (3.31)$$

we obtain

$$\langle \Psi_T | \widehat{H}^2 | \Psi_T \rangle = \int d\tau \Psi_T^*(\tau) \Psi_T(\tau) |E_{Loc}(\tau)|^2, \quad (3.32)$$

and therefore

$$\frac{\langle \Psi_T | \widehat{H}^2 | \Psi_T \rangle}{\langle \Psi_T | \Psi_T \rangle} = \frac{\int d\tau \Psi_T^*(\tau) \Psi_T(\tau) |E_{Loc}(\tau)|^2}{\int d\tau \Psi_T^*(\tau) \Psi_T(\tau)}. \quad (3.33)$$

The computation of the variance of energy, Eq. (3.21), has thus been reduced to two integrals, Eqs. (3.26) and (3.33), both of which involving the same local energy,  $E_{Loc}$ , that one encounters in standard VMC. It is clear that the formulation and the equations in this section are applicable to both bosons and fermions.

### 3.2.4 Universal equation of state at the Van der Waals length scale for $N$ Bose atoms in a symmetric harmonic trap

For any state in which the atomic interaction at the average atomic separation is well represented by  $-C_6/r^6$ , which for  $N$  Bose atoms in a trap implies  $\rho\beta_6^3 \sim N(\beta_6/a_{ho})^3 < \sim 10$ , its energy follows a universal behavior [11, 19] that is uniquely determined by the trapping and the Van der Waals potentials, independent of the interactions at short distances except through a parameter that can be taken either as the short range K matrix  $K^c$  [5] or the  $s$  wave scattering length  $a_0$ . Within the VMC formulation, this can be understood by noting that for such diffuse states, the

solution  $u_\lambda(r)$  of Eq. (4.32), wherever it has an appreciable value [30], is given by [5, 11, 6, 19]

$$u_{\lambda_s}(r_s) = B[f_{\lambda_s l=0}^{c(6)}(r_s) - K^c g_{\lambda_s l=0}^{c(6)}(r_s)]. \quad (3.34)$$

Here  $B$  is a normalization constant and  $f_{\lambda_s l}^{c(6)}$  and  $g_{\lambda_s l}^{c(6)}$  are universal AQDT reference functions for  $-C_6/r^6$  potential [31, 5, 11]. They depend on  $r$  only through a scaled radius  $r_s = r/\beta_6$ , and on energy only through a scaled energy  $\lambda_s = \lambda/s_E$ , where  $s_E = (\hbar^2/m)(1/\beta_6)^2$  is the energy scale associated with the Van der Waals interaction.  $K^c$  is a short-range K matrix [5] that is related to the  $s$  wave scattering length  $a_0$  by [30, 6]

$$a_0/\beta_6 = \left[ b^{2b} \frac{\Gamma(1-b)}{\Gamma(1+b)} \right] \frac{K^c + \tan(\pi b/2)}{K^c - \tan(\pi b/2)}, \quad (3.35)$$

where  $b = 1/(n-2)$ , with  $n = 6$ . Note that while  $K^c$  and  $a_0$  are related to each other, by propagating the wave function in the Van der Waals potential from small to large distances [32, 6], they have considerably different physical meanings.  $K^c$  is a short-range parameter that is directly related to the logarithmic derivative of the wave function coming out of the inner region, a region where the atomic interaction may differ from  $-C_6/r^6$  [5].  $a_0$  is determined by the asymptotic behavior of the wave function at large distances. The universal behavior is conceptually easier to understand in terms of  $K^c$ , as it simply implies that for any state in which the probability for finding particles in the inner region is small, the only role of the inner region is in determining the logarithmic derivative of the wave function coming out of it. The results are presented in terms of a scaled  $a_0$  parameter only to facilitate connections with existing models and understandings.

When  $u_\lambda$ , as given by Eq. (4.35), and therefore  $F$ , depends on the interactions of shorter range than  $\beta_6$  only through  $K^c$  or a scaled  $a_0$ , so do the overall wave function and the energy of the  $N$ -atom Bose system. For an inhomogeneous system of atoms in a trap, the energy depends of course also on the trap configuration. To be specific, I consider here atoms in a symmetric harmonic trap, characterized by

$$V_{ext}(r) = \frac{1}{2}m\omega^2r^2, \quad (3.36)$$

where  $\omega$  is the trap frequency. The corresponding independent-particle solution suggests

$$\phi(\mathbf{r}) = \exp \left[ -\alpha(r/a_{ho})^2 \right], \quad (3.37)$$

where  $\alpha$  is chosen as one of the variation parameters, in addition to parameters  $d$  and  $\gamma$  used to characterize the correlation function  $F$ . From this combination of  $\phi$  and  $F$ , the resulting VMC energy per particle, properly scaled, can be written as

$$\frac{E/N}{\hbar\omega} = \Omega(a_0/a_{ho}, \beta_6/a_{ho}), \quad (3.38)$$

where  $\Omega$  is a universal function that is uniquely determined by the number of particles, the exponent of the Van der Waals interaction ( $n = 6$ ), and the exponent of the trapping potential (2 for the harmonic trap). The strengths of interactions, as characterized by  $C_6$  and  $\omega$ , play a role only through scaling parameters such as  $\beta_6$  and  $a_{ho}$ .

Equation (3.38), which is one example of what we call the universal equation of

state at length scale  $\beta_6$ , can also be defined, independent of the VMC formulation, using the method of effective potential as in Ref. [11]. It is a method of renormalization in the coordinate space to eliminate all length scales shorter than  $\beta_6$ . The same procedure in VMC corresponds simply to using Eq. (4.35) for all  $r < d$  (see Appendix C). The function  $\Omega$ , following this procedure, is rigorously defined for all values of  $a_0/a_{ho}$  and for all  $\beta_6/a_{ho} > 0$ . An  $N$ -atom Bose system in a symmetric harmonic trap and in the lowest gaseous BEC state can be expected to follow this universal behavior for  $\beta_6/a_{ho} < \sim 2/N^{1/3}$ , beyond which the interactions of shorter range, such as  $-C_8/r^8$ , can be expected to come into play.

It is worth noting that the parameter  $\beta_6/a_{ho}$  in Eq. (3.38) plays a similar role, for atoms in a trap, as  $\rho\beta_6^3$  for homogeneous systems [11, 19]. The latter parameter is not used here because  $\rho$  is not uniform, but its order of magnitude is still related to  $\beta_6/a_{ho}$  by  $\rho\beta_6^3 \sim N(\beta_6/a_{ho})^3$ . When either parameter goes to zero, the universal equations of state at length scale  $\beta_6$  can be expected to go to the shape-independent results as obtained by Blume and Greene [1] for particles in a trap and by Giorgini *et al.* [2] for homogeneous systems [11, 19].

# Chapter 4

## Results

### 4.1 Testing

As with all algorithms, a certain amount of testing must be undertaken in order to gain the confidence required to go out and investigate a new problem. In order to be of any use the tests must be able to reproduce previously accepted results to at least the same degree of accuracy.

#### 4.1.1 Hard Spheres in a Trap

The first test of the algorithm involved placing a few particles which behaved as hard spheres, of radius  $a$ , in a spherically symmetric harmonic trap. This is a very good initial test as Diffusion Monte Carlo (DMC) results are available [1] in order to do a comparison. Hard spheres interact via the potential,

$$v_{int}(r) = \begin{cases} \infty & , \quad r \leq a \\ 0 & , \quad r > a \end{cases} , \quad (4.1)$$

where  $a$  is the size of the hard sphere. In the dilute limit the the hard sphere potential may be approximated by the contact potential,

$$v(r) = \frac{4\pi\hbar^2 a}{m} \delta(r) = g\delta(r) , \quad (4.2)$$

whose scattering in this limit is purely s-wave with scattering length  $a_0$ , with  $a = a_0$ . For hard spheres the s-wave scattering length,  $a_0$ , is always positive hence a repulsive interaction. Since the particles are in a symmetric trap the interaction potential becomes,

$$V_{ext}(\mathbf{r}) = \frac{1}{2} m \omega_{ho}^2 r^2 . \quad (4.3)$$

We use a Jastrow wavefunction of the form Eq (3.6), with

$$\phi(r) = \exp(-\alpha r^2) , \quad (4.4)$$

where  $\alpha$  is a variational parameter and the correlation,  $F(r)$ , term is given by Eq (3.19). The local energy,  $E_{Loc}$ , may now be expressed as,

$$E_L^{(1)} = 3\alpha + \frac{1}{2} (1 - 4\alpha^2) r_1^2 , \quad (4.5)$$

$$E_{L1}^{(2)} = 0, \quad (4.6)$$

$$E_{L2}^{(2)} = (N - 1)\alpha \frac{r_1^2 - r_2^2 + r_{12}^2}{r_{12}^2 [(r_{12}/a) - 1]}, \quad (4.7)$$

and

$$E_L^{(3)} = -\frac{1}{4}(N - 1)(N - 2) \frac{r_{12}^2 + r_{13}^2 - r_{23}^2}{r_{12}^2 r_{13}^2 [(r_{12}/a) - 1] [(r_{13}/a) - 1]}. \quad (4.8)$$

Once the local energy and the wavefunction have been defined then one may perform a numerical computation using the ideas outlined in appendix A. Figure 4-1 illustrates the results for the energy of two interacting hard spheres in a harmonic spherical trap, as a function of  $a_0/a_{ho}$ . As the figure shows the VMC results agree well with the DMC and they both show that the ground state energy for two hard spheres is dependent on the s-wave scattering length  $a_0$ . The ground state energy for non-interacting particles is  $E/N = 1.5\hbar\omega$ .

Figures 4-2 and 4-3 display the results for few and many hard spheres in a harmonic trap. As is the case with two interacting hard spheres the VMC results for few and many hard spheres in a trap produce VMC results which agree well with the DMC results. The Complete set of data are presented in Tables B.1, B.2 and B.3 from appendix B.

### 4.1.2 Homogeneous Bose System

The second test involved a large number of interacting hard spheres, of radius  $a$ , in a homogeneous system, i.e. no external trap,  $V_{ext} = 0$ , therefore  $\phi = 1$ . For such a

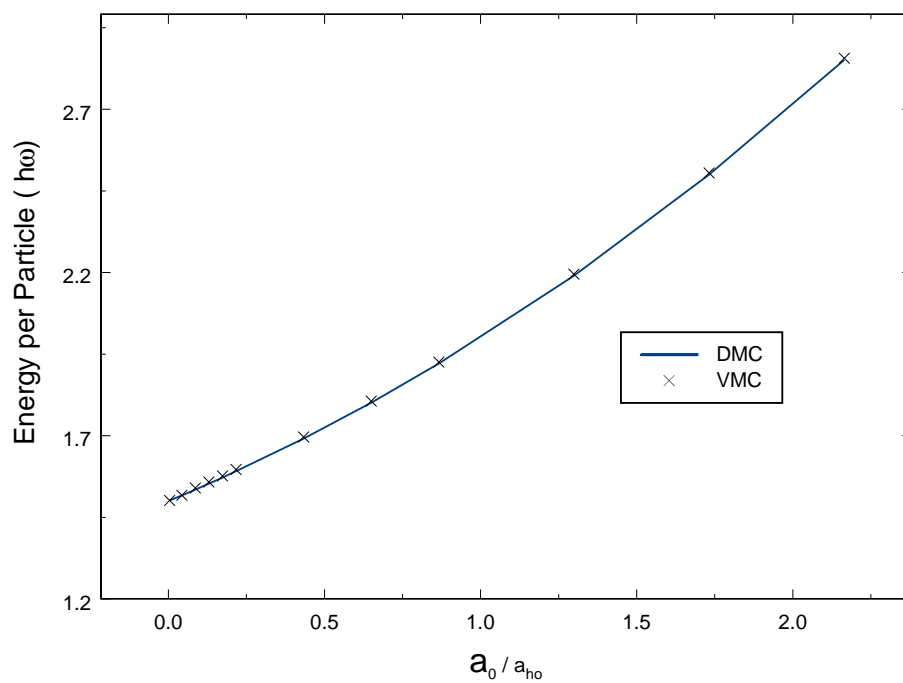


Figure 4-1: A comparison of the DMC[1] and VMC values for two hard spheres in a symmetric harmonic trap.

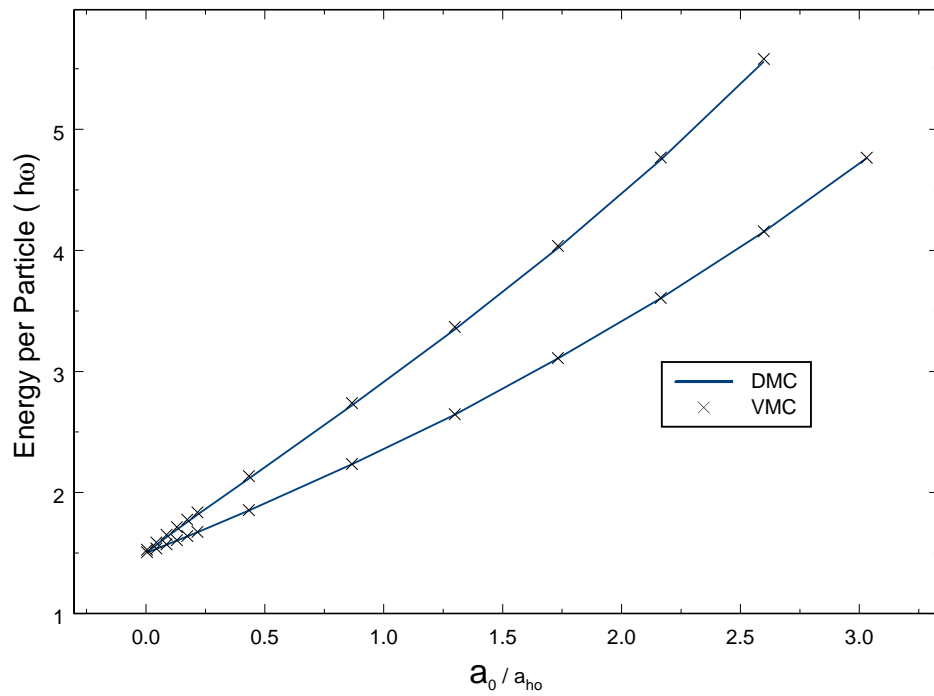


Figure 4-2: A comparison of the DMC[1] and VMC values for  $N = 3$  (lower curve) and  $N = 5$  (upper curve) hard spheres in a symmetric harmonic trap.

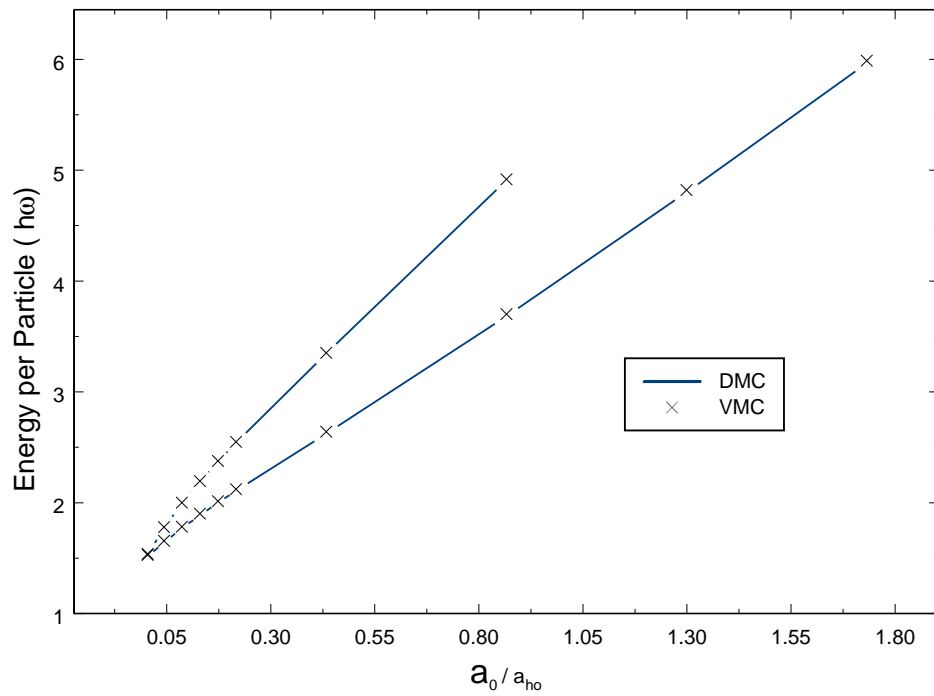


Figure 4-3: A comparison of the DMC[1] and VMC values for  $N = 10$  (lower curve) and  $N = 20$  (upper curve) hard spheres in a symmetric harmonic trap.

system the wavefunction is expressed as,

$$\Psi = \prod_{i < j=1}^N F(r_{ij}). \quad (4.9)$$

The local energy, for this system, is expressed as,

$$E_{Loc} = E_{L1}^{(2)}(\mathbf{r}_1, \mathbf{r}_2) + E_L^{(3)}(\mathbf{r}_1, \mathbf{r}_2, \mathbf{r}_3). \quad (4.10)$$

The *healing distance*,  $d$ , is introduced as a variational parameter which satisfies the condition,

$$\frac{1}{F} \left( -\frac{\hbar^2}{2\mu} \nabla^2 \right) F + v = \begin{cases} \epsilon & , \quad r \leq d \\ v(r) & , \quad r > d \end{cases}. \quad (4.11)$$

Whereas  $F$  is represented by,

$$F(r) = \begin{cases} A \frac{1}{r} \sin \{k(r - a)\} & , \quad r \leq d \\ 1 & , \quad r > d \end{cases}, \quad (4.12)$$

and  $F'(d) = 0$ . Applying the boundary conditions to  $F(r)$  one is able to determine a value for the constant  $A$ ,

$$A = \frac{d}{\sin \{k(d - a)\}} \quad (4.13)$$

and applying the boundary condition to its derivative we arrive at the equation,

$$\tan \{k(d - a)\} = kd. \quad (4.14)$$

Here  $k$  is related to  $\epsilon$  by the equation,

$$\epsilon = \frac{\hbar^2}{2\mu} k^2, \quad (4.15)$$

The local energy,  $E_{Loc}$ , is now expressed as,

$$E_{L1}^{(2)} = \frac{1}{2}(N-1) \begin{cases} \epsilon & , \quad r \leq d \\ 0 & , \quad r > d \end{cases}, \quad (4.16)$$

and

$$E_L^{(3)} = -(N-1)(N-2) \left(-\frac{\hbar^2}{2m}\right) \left[ \frac{F'(r_{12})}{F(r_{12})} \right] \left[ \frac{F'(r_{13})}{F(r_{13})} \right] \frac{r_{12}^2 + r_{13}^2 - r_{23}^2}{2r_{12}r_{13}}, \quad (4.17)$$

with,

$$\frac{F'(r)}{F(r)} = \begin{cases} -\frac{1}{r} + k \cot \{k(r-a)\} & , \quad r \leq d \\ 0 & , \quad r > d \end{cases}, \quad (4.18)$$

As Figure 4-4 shows, the DMC results and the VMC results are in excellent agreement for a range of densities.

This concludes the testing phase of the algorithm, both of which are very successful.

## 4.2 Few Atoms in a Trap

The wavefunction for this system is of the form Eq (3.6), with

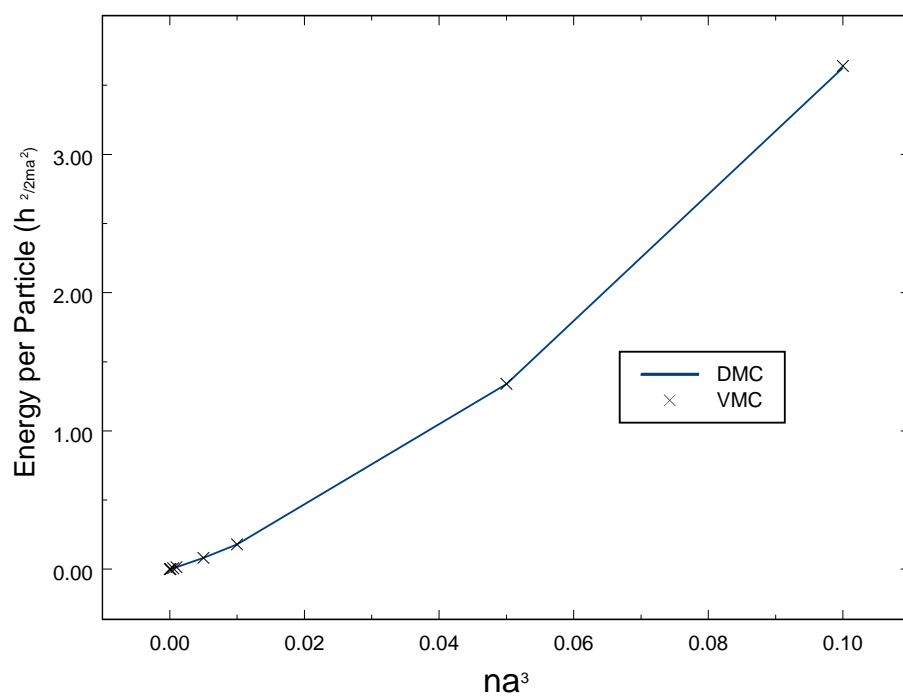


Figure 4-4: A comparison of the DMC[2] and VMC values for hard spheres in a homogeneous system.

$$\phi(r) = \exp(-\alpha r^2), \quad (4.19)$$

in similar fashion to section (4.1.1) and the correlation function,  $F(r)$ , is given by Eq (3.17). The local energy,  $E_{Loc}$ , is now given by,

$$E_L^{(1)} = 3\alpha + \frac{1}{2} (1 - 4\alpha^2) r_1^2, \quad (4.20)$$

$$E_{L1}^{(2)} = \frac{1}{2}(N-1) \begin{cases} \epsilon & , \quad r_{12} \leq d \\ -\frac{1}{r_{12}^6} & , \quad r_{12} > d \end{cases}, \quad (4.21)$$

$$E_{L2}^{(2)} = \alpha(N-1) \frac{r_1^2 - r_2^2 + r_{12}^2}{r_{12}} \begin{cases} \left[ \frac{u'_\lambda}{u_\lambda} - \frac{1}{r_{12}} \right] & , \quad r_{12} \leq d \\ \frac{\gamma}{r_{12}} & , \quad r_{12} > d \end{cases}, \quad (4.22)$$

and

$$E_L^{(3)} = -\frac{1}{2}(N-1)(N-2) \frac{r_{12}^2 + r_{13}^2 - r_{23}^2}{r_{12}r_{13}} \left| \frac{\nabla f(r_{12})}{f(r_{12})} \right| \left| \frac{\nabla f(r_{13})}{f(r_{13})} \right|. \quad (4.23)$$

With,

$$\left| \frac{\nabla f(r)}{f(r)} \right| = \begin{cases} \left[ \frac{u'_\lambda}{u_\lambda} - \frac{1}{r} \right] & , \quad r \leq d \\ \frac{\gamma}{r} & , \quad r > d \end{cases}, \quad (4.24)$$

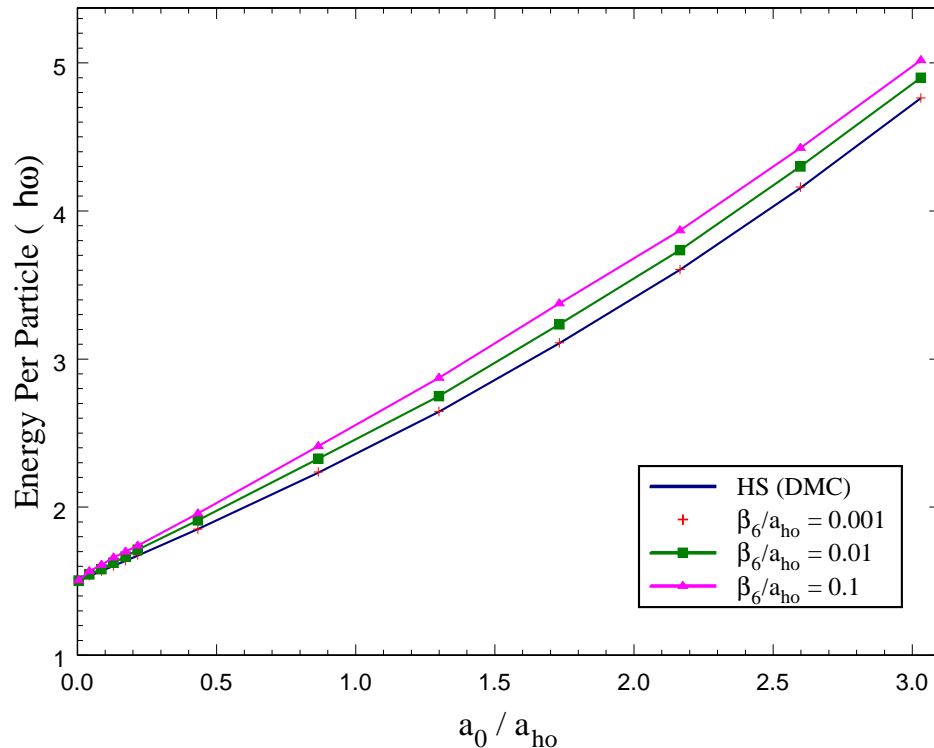


Figure 4-5: The universal equation of state for three atoms in a symmetric harmonic trap as a function of  $a_0/a_{ho}$ , compared to the DMC results of Blume and Greene for hard spheres [1].

#### 4.2.1 Positive Scattering Length

Results are presented for few Bose atoms in a symmetric harmonic trap with  $a_0 > 0$ . This is not only because such calculations are less numerically intensive than for a larger number of atoms, but also because (before  $N$  gets sufficiently large that  $\rho\beta_6^3 \sim 1$ ) the shape-dependent confinement correction is actually more important for smaller number of particles [33].

Figure 4-5 illustrates the equation of state for three atoms in a symmetric harmonic trap. It is a function of two variables that we plot here as a set of functions of  $a_0/a_{ho}$

for different values of  $\beta_6/a_{ho}$ . The results for  $\beta_6/a_{ho} = 0.001$  show that, as expected, the universal equation of state at length scale  $\beta_6$  does *eventually* approach a shape-independent result in the limit of  $\beta_6/a_{ho} \rightarrow 0$ , and are in excellent agreement with the DMC results of Blume and Greene for hard spheres [1]. The results for  $\beta_6/a_{ho} = 0.01$  and  $\beta_6/a_{ho} = 0.1$  illustrate the shape-dependence of the equation of state due to the Van der Waals interaction. They show that even for relative small  $\rho\beta_6^3$ , which is of order of  $10^{-6}$  for  $\beta_6/a_{ho} = 0.01$ , the shape-dependent correction can become quite appreciable under strong confinement. This correction, which we call the shape-dependent confinement correction [33], can be understood qualitatively as due to energy dependence of the two-body scattering amplitude [34, 35, 36, 33, 27], which becomes significant for large scattering lengths. To put the results in perspective, we note that a recent experiment on two atoms in a symmetric harmonic trap is already exploring the region close to  $\beta_6/a_{ho} \sim 0.1$  [37].

Figure 4-6 shows that the parameter  $\gamma$ , characterizing the long-range atomic correlation, for three atoms in a symmetric harmonic trap. It is clear that  $\gamma$  can become quite large under strong confinement,  $a_0/a_{ho} \sim 1$ . Not surprisingly, a variational wave function that does not incorporate this long-range correlation explicitly would fail under such conditions.

Figure 4-7 shows the equation of states for five atoms in a symmetric harmonic trap. Compared to the results for three atoms, the shape-dependent corrections can be seen to be less significant, confirming the conclusion that the shape-dependent confinement correction is more important for smaller number of particles than for larger number of particles [33]. The long-range atom-atom correlation is again very

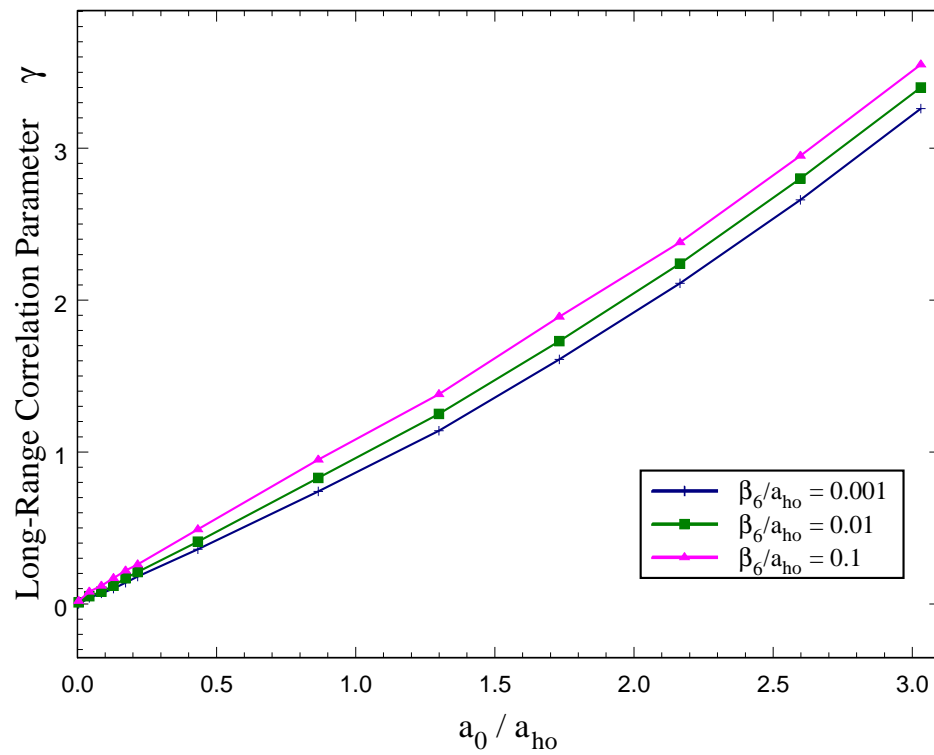


Figure 4-6: The parameter  $\gamma$ , characterizing the long-range atom-atom correlation, for three atoms in a symmetric harmonic trap, as a function of  $a_0/a_{ho}$ .

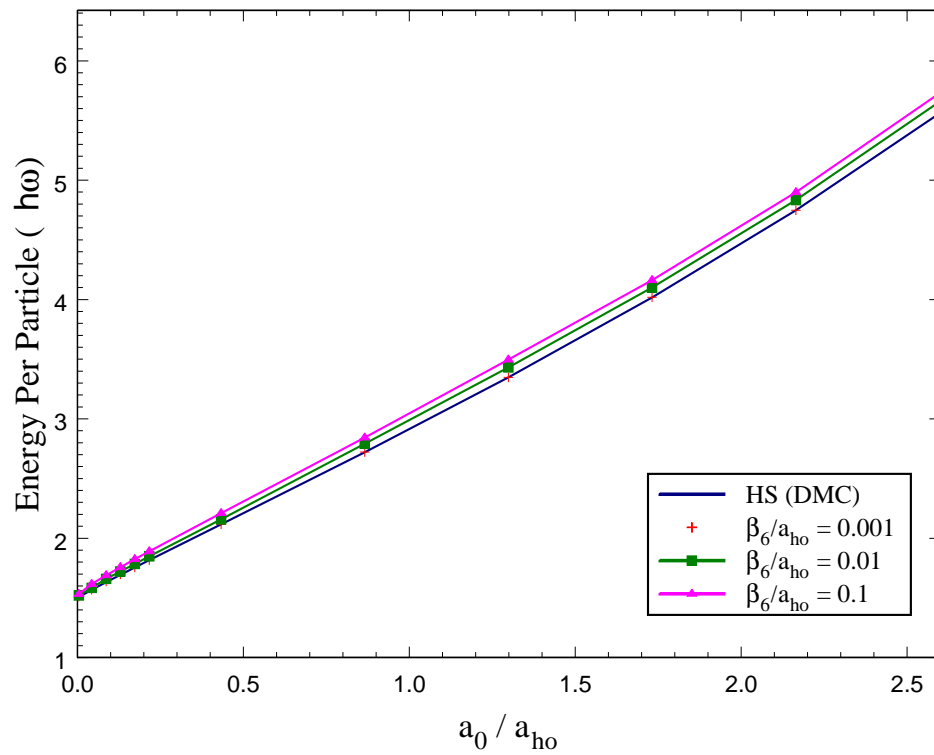


Figure 4-7: The universal equation of state for five atoms in a symmetric harmonic trap as a function of  $a_0/a_{ho}$ , compared to the DMC results of Blume and Greene for hard spheres [1].

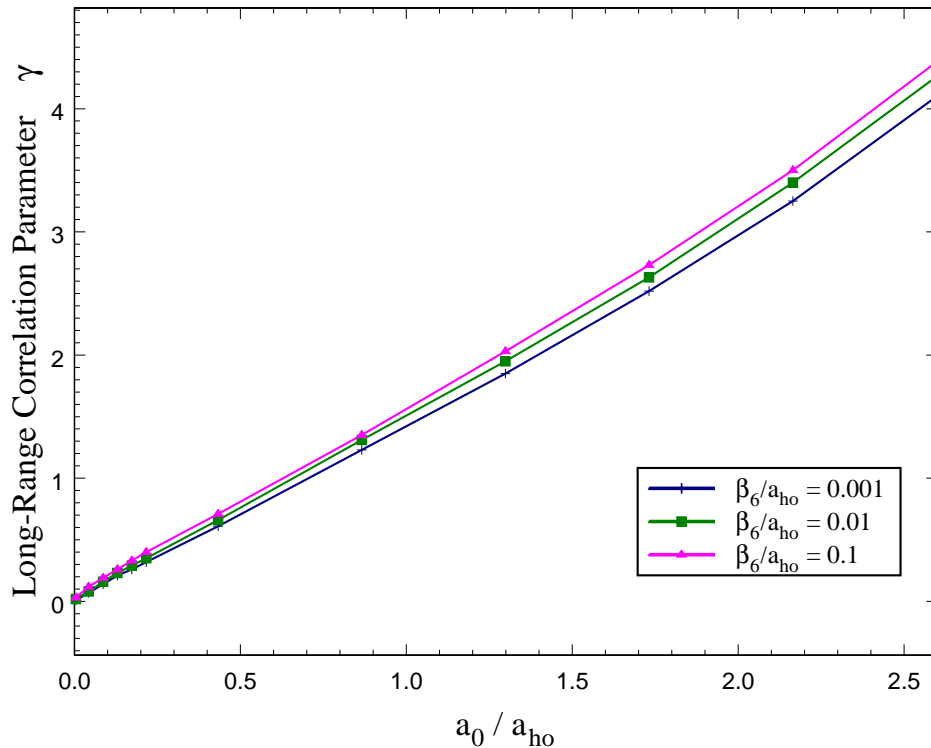


Figure 4-8: The parameter  $\gamma$ , characterizing the long-range atom-atom correlation, for five atoms in a symmetric harmonic trap, as a function of  $a_0/a_{ho}$ .

important, as shown in Figure 4-8.

### 4.2.2 Negative Scattering Length

Atoms with negative scattering length  $a_0 < 0$ , display a different behaviour to that of positive scattering length. The equation of state is described in exactly the same manner as the repulsive interactions with only  $a_0$  being expressed as a negative number. The results of the computation are presented in Figure (4-9), for  $N = 3$ , and Figure (4-10) for  $N = 5$ . Both graphs show that the Energy per particle reaches

a plateau very quickly when  $a_0 < 0$ .

One of the interesting features of both graphs is that it was not possible to obtain results after a specific value for the scattering length. For the case of  $N = 3$  it was not possible to compute the energy per particle for  $\frac{|a_0|}{a_{ho}} > 1.5$  while for the case of  $N = 5$  it was not possible to compute the energy for  $\frac{|a_0|}{a_{ho}} > 1$ . This suggest that the system of particles with an attractive interaction becomes unstable, when  $a_0 \simeq a_{ho}$ , and results in a collapse. This collapse is due to the collective behaviour of the system as a result of negative pressure.

Also the variational parameter associated with the long range correlation,  $\gamma$ , was found to be of little significance, for most of the results it was found  $\gamma \simeq 0$ . This strongly suggests that  $F(r)$  takes the form,

$$F(r) = \begin{cases} \frac{u\lambda}{r} & , \quad r \leq d \\ 1 & , \quad r > d \end{cases} , \quad (4.25)$$

However, in a similar fashion to the positive scattering length, the shape dependent confinement correction was found to be more important for  $N = 3$  than it is for  $N = 5$ .

### 4.3 Homogeneous Bose Gas

A homogeneous Bose gas is a system of many particles with no external trap,  $V_{ext} = 0$ . This makes  $\Phi = 1$  and  $F(r)$  is given by Eq (3.17). Therefore the local energy,  $E_{Loc}$  is only composed of two terms,

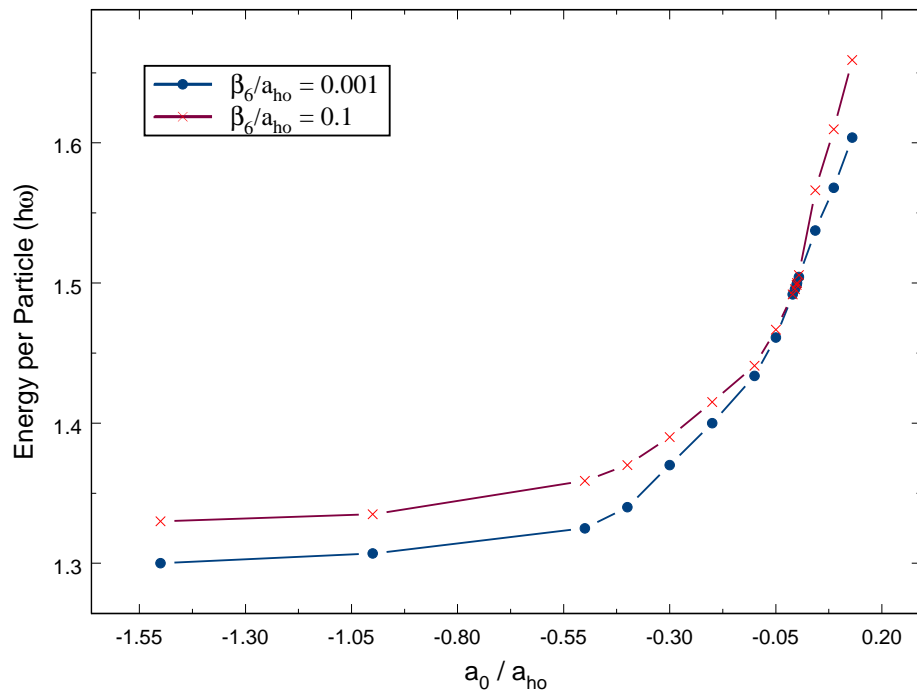


Figure 4-9: The universal equation of state for three atoms in a symmetric harmonic trap as a function of  $a_0/a_{ho}$ , with negative scattering length.

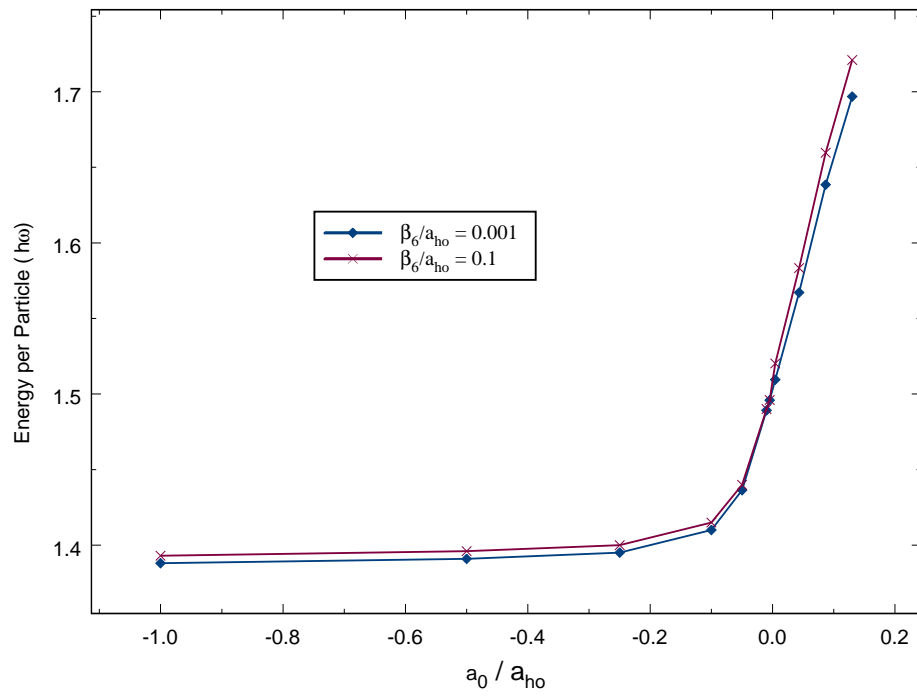


Figure 4-10: The universal equation of state for five atoms in a symmetric harmonic trap as a function of  $a_0/a_{ho}$ , with negative scattering length.

$$E_{L1}^{(2)} = \frac{1}{2}(N-1) \begin{cases} \epsilon & , r_{12} \leq d \\ -\frac{1}{r_{12}^6} & , r_{12} > d \end{cases} , \quad (4.26)$$

and

$$E_L^{(3)} = -\frac{1}{2}(N-1)(N-2) \frac{r_{12}^2 + r_{13}^2 - r_{23}^2}{r_{12}r_{13}} \left| \frac{\nabla f(r_{12})}{f(r_{12})} \right| \left| \frac{\nabla f(r_{13})}{f(r_{13})} \right|. \quad (4.27)$$

With,

$$\left| \frac{\nabla f(r)}{f(r)} \right| = \begin{cases} \left[ \frac{u'_\lambda}{u_\lambda} - \frac{1}{r} \right] & , r \leq d \\ \frac{\gamma}{r} & , r > d \end{cases} . \quad (4.28)$$

Once the local energy has been established one may compute the equation of state, in this simulation  $N = 256$ . Figures (4-11) and (4-12) display the VMVMC results as compared to the nearest neighbor result of [11] for both positive and negative scattering lengths. As the figures show, for the densities and scattering lengths involved, the VMVMC performed very well when compared to the nearest-neighbor theory (NNT). A typical variance of  $\Delta E/E \leq 10^{-3}$  was found.

However, at much larger densities,  $\rho_s > 1$ , the VMVMC did not perform very well when compared to the nearest neighbour theory, a typical variance of,  $\Delta E/E > 10^{-2}$  was found.

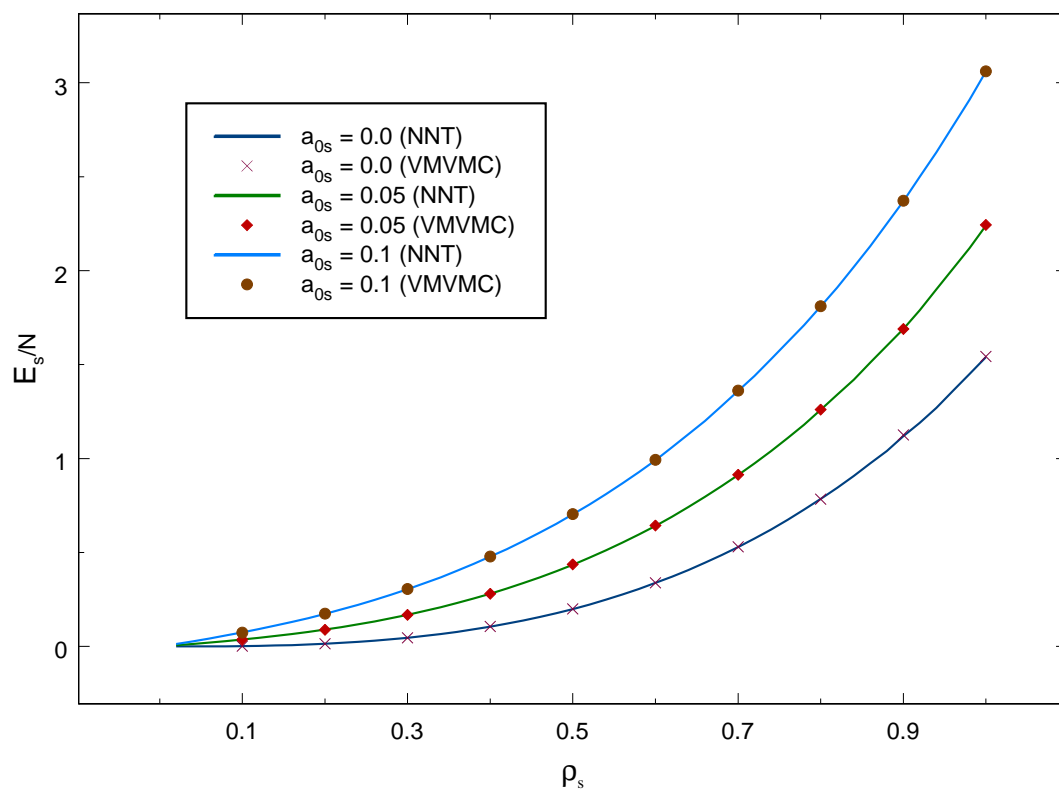


Figure 4-11: Positive scattering length.

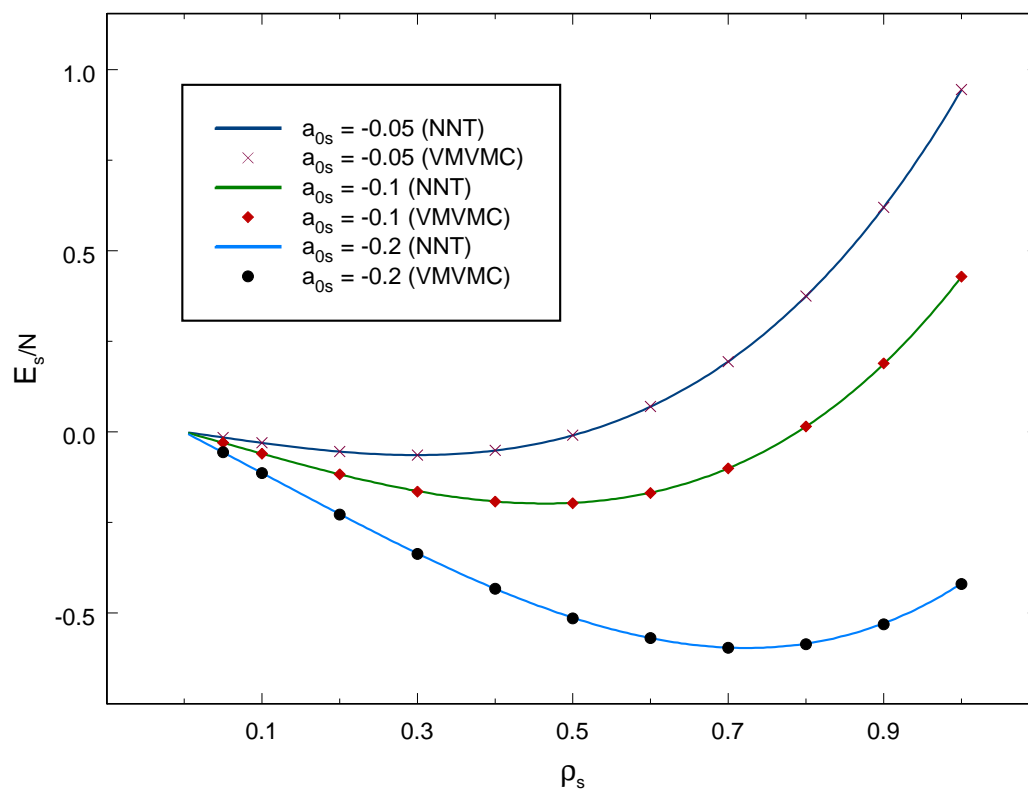


Figure 4-12: Negative scattering length.

## 4.4 Excited states

The VMVMC, as outlined in Section (3.2.3), was first applied in Ref. [12] to study the universal equation of state at the van der Waals length scale [11, 19] for few identical Bose atoms ( $N = 3-5$ ) in a trap. To better illustrate and to further test the method, we investigate here the universal spectrum at the van der Waals length scale for two identical Bose atoms in a symmetric harmonic trap. It is a problem for which accurate results can be obtained independently using a variety of methods [38, 34, 35, 36], including a multiscale QDT [27, 3].

Two identical Bose atoms in a symmetric harmonic trap are described by the Hamiltonian, Eqs. (3.24)-(3.25), with  $N = 2$ , and

$$V_{ext}(\mathbf{r}_i) = \frac{1}{2}m\omega^2 r_i^2, \quad (4.29)$$

where  $m$  is the mass of an atom, and  $\omega$  is the trap frequency.

For the trap states of interest here, we take the trial wave function to be of the form of

$$\Psi_T = [\phi_1(\mathbf{r}_1)\phi_2(\mathbf{r}_2) + \phi_1(\mathbf{r}_2)\phi_2(\mathbf{r}_1)] F(r_{12}), \quad (4.30)$$

where  $\phi_1$  and  $\phi_2$  are independent-particle orbitals, and  $F$  is the atom-atom correlation function that is discussed in more detail in Ref. [12]. Specifically, we use

$$F(r) = \begin{cases} Au_\lambda(r)/r & , \quad r < d \\ (r/d)^\gamma & , \quad r \geq d \end{cases}, \quad (4.31)$$

where  $u(r)$  satisfies the Schrödinger equation:

$$\left[ -\frac{\hbar^2}{m} \frac{d^2}{dr^2} + v(r) - \lambda \right] u_\lambda(r) = 0, \quad (4.32)$$

for  $r < d$ .  $\gamma$  is the parameter characterizing the long-range correlation between atoms in a trap, with  $\gamma = 0$  (meaning  $F = 1$  for  $r > d$ ) corresponding to no long-range correlation. Both  $d$  and  $\gamma$  are taken to be variational parameters, in addition to the variational parameters associated with the descriptions of  $\phi_1$  and  $\phi_2$ . The parameters  $A$  and  $\lambda$  are not independent. They are determined by matching  $F$  and its derivative at  $d$ . Our choice of  $F$  differs from traditional choices (see, e.g. Ref. [17]) not only in its treatment of the short-range correlation, but especially in its allowance for the long-range correlation characterized by parameter  $\gamma$ . This was first suggested by a multiscale QDT treatment of two atoms in a symmetric harmonic trap [27, 3], and was later found to be the key for treating  $N$  trapped atoms in cases of strong coupling, namely when the  $s$  wave scattering length  $a_0$  becomes comparable to or greater than the trap length scale  $a_{ho} = (\hbar/m\omega)^{1/2}$  [12].

For atoms in their ground state, the atom-atom interaction is of the van der Waals type of  $-C_n/r^n$  with  $n = 6$  at large interatomic separations, i.e.,

$$v(r) \xrightarrow{r \rightarrow \infty} -C_6/r^6. \quad (4.33)$$

This interaction has an associated length scale of  $\beta_6 = (mC_6/\hbar^2)^{1/4}$ , and a corresponding energy scale of  $s_E = (\hbar^2/m)(1/\beta_6)^2$  [31]. Over a wide range of energies that

is hundreds of  $s_E$  around the threshold [5, 39], the details of atomic interactions of shorter range than  $\beta_6$  are not important, and can be characterized by a single parameter that can be the  $s$  wave scattering length  $a_0$ , the short range  $K$  matrix  $K^c$ , or some other related parameters [40, 5, 6]. In this range of energies, the spectrum of two atoms in a trap follows a universal property that can be characterized by [12, 27, 3]

$$\frac{E_i/N}{\hbar\omega} = \Omega_i(a_0/a_{ho}, \beta_6/a_{ho}) , \quad (4.34)$$

and is called the universal spectrum at length scale  $\beta_6$ . Here  $\Omega_i$  are universal functions that are uniquely determined by the number of particles, the exponent of the van der Waals interaction ( $n = 6$ ), and the exponent of the trapping potential (2 for the harmonic trap). The strengths of interactions, characterized by  $C_6$  and  $\omega$ , play a role only through scaling parameters such as  $\beta_6$  and  $a_{ho}$ .

As in Ref. [12], the universal spectrum at length scale  $\beta_6$ , namely the  $\Omega_i$ 's in Eq. (4.34), can be computed by using a correlation function, Eq. (3.17), with  $u_\lambda(r)$  as given by the angular-momentum-insensitive quantum-defect theory (AQDT) [5],

$$u_{\lambda_s}(r_s) = B[f_{\lambda_s l=0}^{c(6)}(r_s) - K^c g_{\lambda_s l=0}^{c(6)}(r_s)] . \quad (4.35)$$

Here  $B$  is a normalization constant.  $f_{\lambda_s l}^{c(6)}$  and  $g_{\lambda_s l}^{c(6)}$  are universal AQDT reference functions for  $-C_6/r^6$  type of potentials [31, 11]. They depend on  $r$  only through a scaled radius  $r_s = r/\beta_6$ , and on energy only through a scaled energy  $\lambda_s = \lambda/s_E$ .  $K^c$  is the short-range  $K$  matrix [5] that is related to the  $s$  wave scattering length  $a_0$  by

[30, 6]

$$a_0/\beta_n = \left[ b^{2b} \frac{\Gamma(1-b)}{\Gamma(1+b)} \right] \frac{K^c + \tan(\pi b/2)}{K^c - \tan(\pi b/2)}, \quad (4.36)$$

where  $b = 1/(n-2)$ , with  $n = 6$ .

Figure 4-5 shows a portion of the universal spectrum at length scale  $\beta_6$  for two Bose atoms in a symmetric harmonic trap. Specifically, it gives the energies of the first three  $s$  wave trap states as a function of  $a_0/a_{ho}$ . The corresponding  $\phi_i$ 's used in Eq. (4.30) are independent-particle orbitals based on standard solutions for a single particle in a symmetric harmonic potential. For the lowest  $s$  wave trap state, they are taken to be

$$\phi_i(\mathbf{r}) = \exp(-\alpha_i x^2), \quad i = 1, 2. \quad (4.37)$$

Also

$$\begin{aligned} \phi_1(\mathbf{r}) &= \exp(-\alpha_1 x^2), \\ \phi_2(\mathbf{r}) &= \left( \frac{3}{2} - x^2 \right) \exp(-\alpha_2 x^2), \end{aligned} \quad (4.38)$$

for the first excited  $s$  wave trap state, and

$$\phi_i(\mathbf{r}) = \left( \frac{3}{2} - x^2 \right) \exp(-\alpha_i x^2), \quad i = 1, 2, \quad (4.39)$$

for the second excited  $s$  wave trap state. Here  $x$  is a scaled radius defined by  $x = r/a_{ho}$ . The variational parameters are  $d$ ,  $\gamma$ ,  $\alpha_1$ , and  $\alpha_2$  in all three cases. The variance of energy is calculated and the minimization is carried out using a type of genetic

algorithm. Since  $N = 2$  for all three cases the local energy is straightforward, for the lowest  $s$  wave trap state,

$$E_L^{(1)} = 3\alpha + \frac{1}{2} (1 - 4\alpha^2) r_1^2, \quad (4.40)$$

$$E_{L1}^{(2)} = \frac{1}{2} \begin{cases} \epsilon & , \quad r_{12} \leq d \\ -\frac{1}{r_{12}^6} & , \quad r_{12} > d \end{cases}, \quad (4.41)$$

$$E_{L2}^{(2)} = \alpha \frac{r_1^2 - r_2^2 + r_{12}^2}{r_{12}} \begin{cases} \left[ \frac{u'_\lambda}{u_\lambda} - \frac{1}{r_{12}} \right] & , \quad r_{12} \leq d \\ \frac{\gamma}{r_{12}} & , \quad r_{12} > d \end{cases}. \quad (4.42)$$

For the first excited state,

$$E_L^{(1)} = 3\alpha - 2r_1^2(\alpha^2 + \alpha + \frac{1}{2}) + \frac{3 - 2\alpha r_1^2}{3 - r_1^2 - r_2^2}, \quad (4.43)$$

$$E_{L1}^{(2)} = \frac{1}{2} \begin{cases} \epsilon & , \quad r_{12} \leq d \\ -\frac{1}{r_{12}^6} & , \quad r_{12} > d \end{cases}, \quad (4.44)$$

$$E_{L2}^{(2)} = 2 \left[ \alpha + \frac{1}{3 - r_1^2 - r_2^2} \right] \frac{r_1^2 - r_2^2 + r_{12}^2}{r_{12}} \begin{cases} \left[ \frac{u'_\lambda}{u_\lambda} - \frac{1}{r_{12}} \right] & , \quad r_{12} \leq d \\ \frac{\gamma}{r_{12}} & , \quad r_{12} > d \end{cases}. \quad (4.45)$$

For the second excited state,

$$E_L^{(1)} = 3\alpha - \frac{r_1^2}{2}(1 - 4\alpha^2) + \frac{3 - 6\alpha r_1^2}{\frac{3}{2} - r_1^2}, \quad (4.46)$$

$$E_{L1}^{(2)} = \frac{1}{2} \begin{cases} \epsilon & , \quad r_{12} \leq d \\ -\frac{1}{r_{12}^6} & , \quad r_{12} > d \end{cases}, \quad (4.47)$$

$$E_{L2}^{(2)} = 2 \left[ \alpha + \frac{1}{3/2 - r_1^2} \right] \frac{r_1^2 - r_2^2 + r_{12}^2}{r_{12}} \begin{cases} \left[ \frac{u'_\lambda}{u_\lambda} - \frac{1}{r_{12}} \right] & , \quad r_{12} \leq d \\ \frac{\gamma}{r_{12}} & , \quad r_{12} > d \end{cases}. \quad (4.48)$$

Both Figs. 4-13 and 4-14 show that the results of VMVMC are in excellent agreements with those of a multiscale QDT [27, 3], which gives basically exact results for two atoms in a symmetric harmonic trap. (The scaled energy per particle,  $E_i/(2\hbar\omega)$ , used here is related to the scaled center-of-mass energy,  $e = \epsilon/\hbar\omega$ , used in Ref. [3], by  $E_i/(2\hbar\omega) = (e + 3/2)/2$ .) The agreements are all within the variances of energy, which are smaller for weaker coupling (smaller  $a_0/a_{ho}$ ) and greater for stronger coupling, but are in any case less than  $1.8 \times 10^{-3}$  for all parameters considered. The results shown in Figure 4-5, which are for a small  $\beta_6/a_{ho} = 0.001$ , illustrate the shape-independent limit of  $\beta_6/a_{ho} \rightarrow 0$  for states with  $E_i/2 \sim \hbar\omega \ll s_E$  [12, 3]. They agree, in this limit, with the results obtained using a delta-function pseudopotential [38]. For greater  $\beta_6/a_{ho}$ , the effects of the van der Waals interaction become gradually more important, especially for strong coupling ( $a_0/a_{ho} \sim 1$  or greater) and for more highly excited states [34, 3]. This is illustrated in Figure 4-7, which compares the results for

$\beta_6/a_{ho} = 0.1$  with those for  $\beta_6/a_{ho} = 0.001$ .

We note that even the lowest trap state is itself a highly excited diatomic state. There are other “molecular” states that are lower in energy [27, 3]. This fact does not, however, lead to any difficulties because VMVMC works the same for the ground and the excited states. It is for the same reason that we were able to investigate the gaseous BEC state for few atoms in a trap [12], which is again a highly excited state. More detailed discussions of the universal spectrum at length scale  $\beta_6$  for two atoms in a symmetric harmonic trap, including the molecular states and the spectra for nonzero partial waves, can be found elsewhere [3].

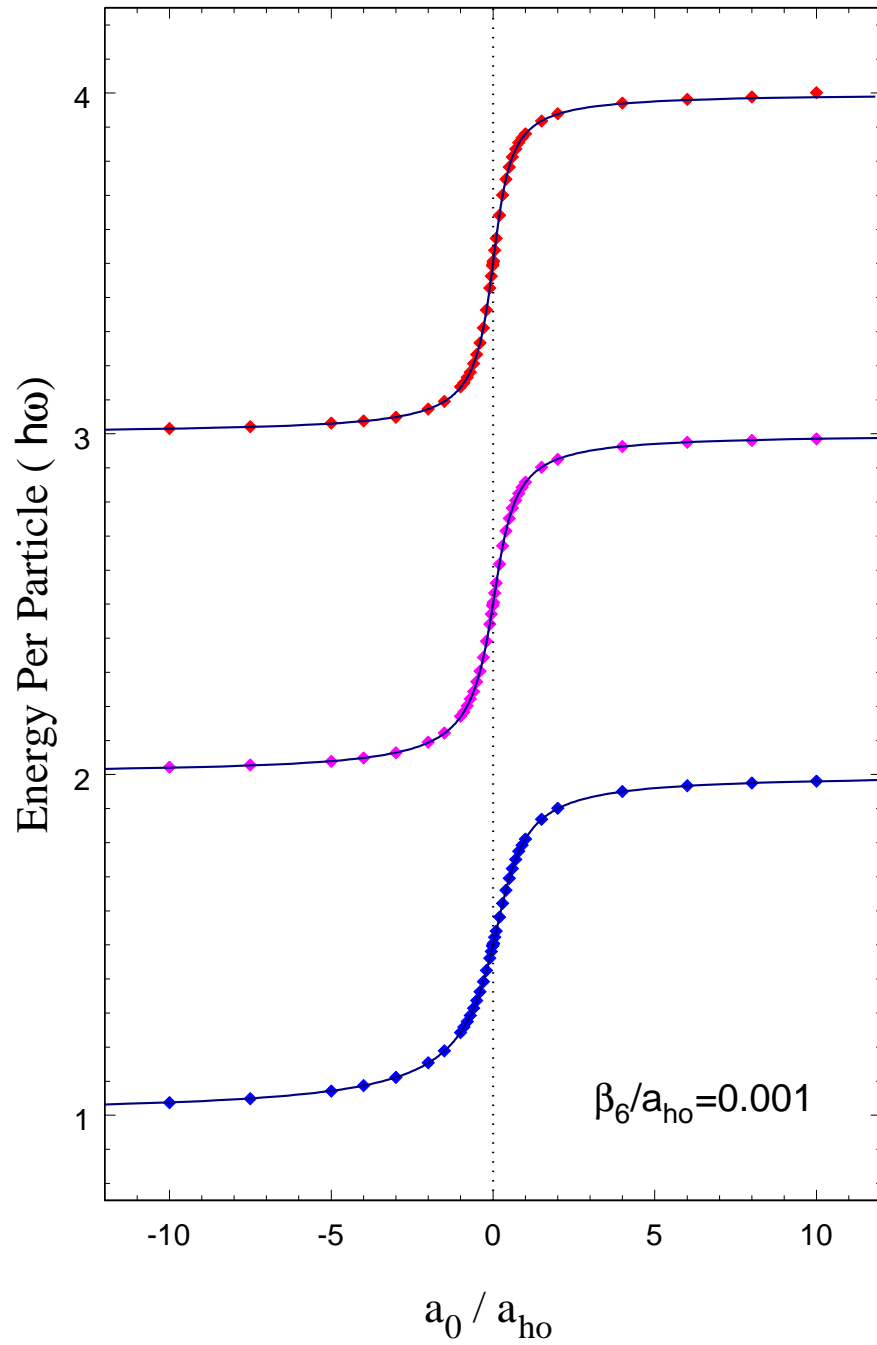


Figure 4-13: The universal spectrum at length scale  $\beta_6$  for two Bose atoms in a symmetric harmonic trap as a function of  $a_0/a_{ho}$  for  $\beta_6/a_{ho} = 0.001$ . Solid line: results from a multiscale QDT [3]. Symbols: results of VMVMC.

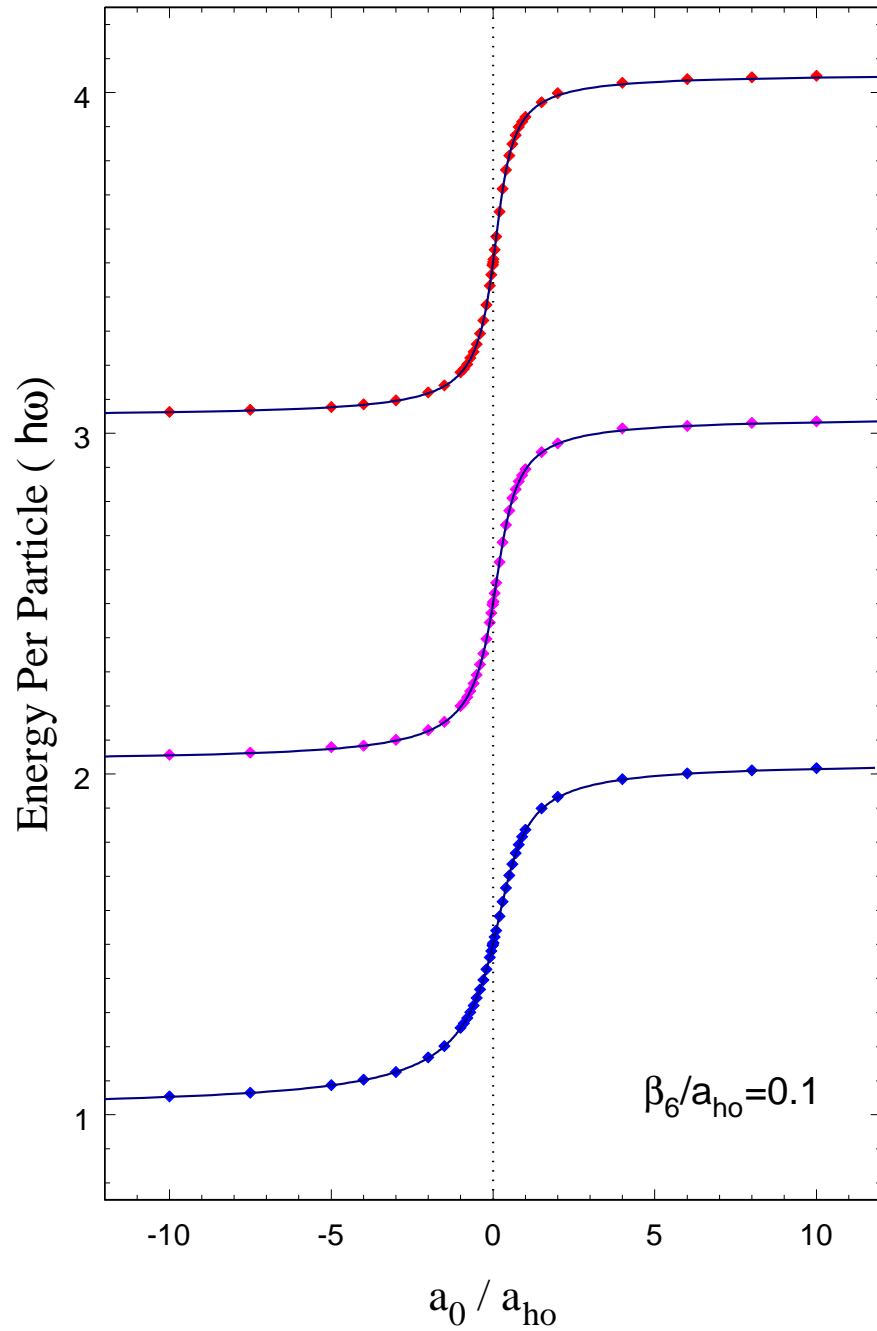


Figure 4-14: The same as Fig. 4-13 except for  $\beta_6/a_{ho} = 0.1$ .

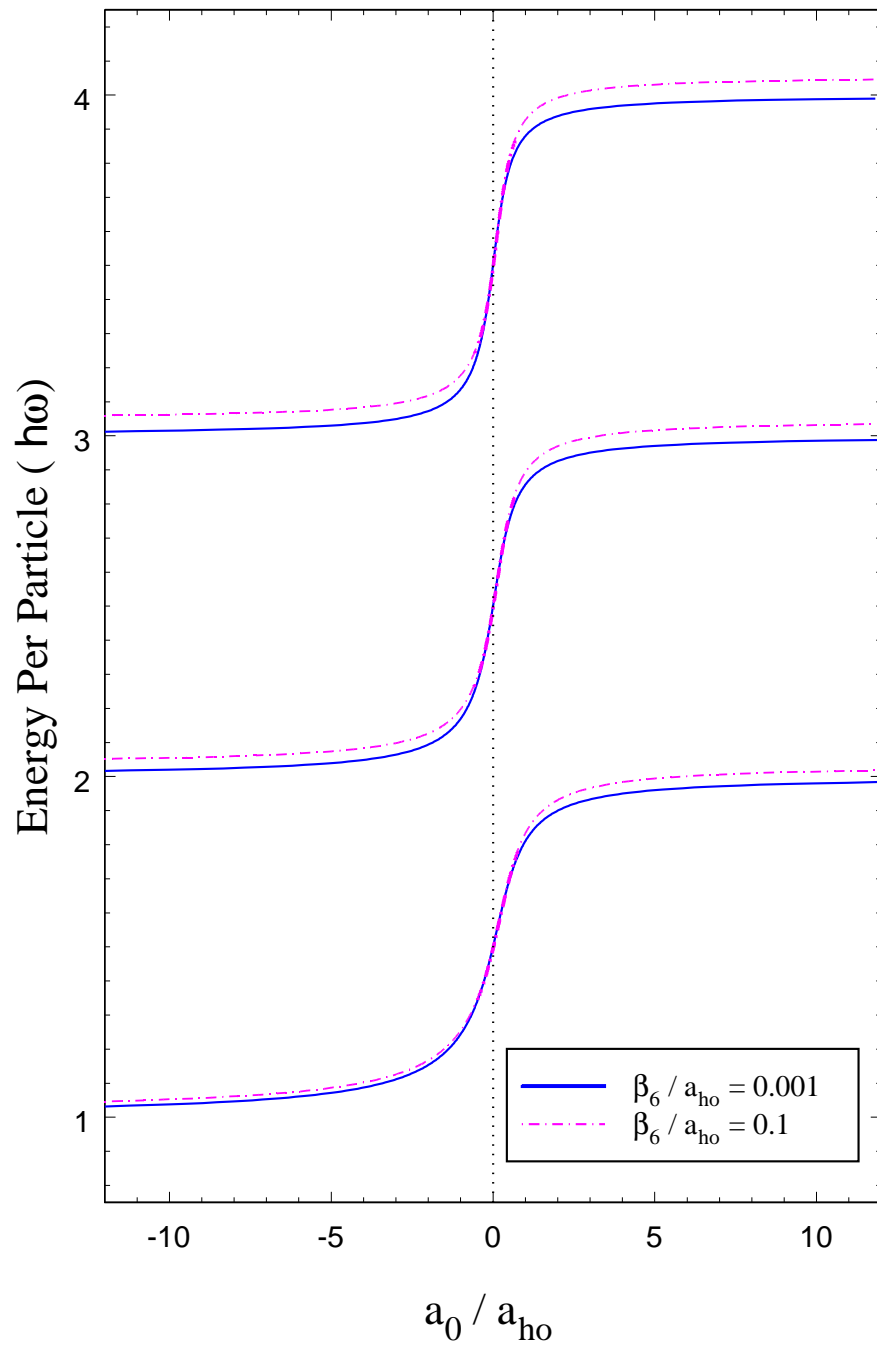


Figure 4-15: A comparison of the spectra for two different values of  $\beta_6/a_{ho}$ , illustrating the shape-dependent correction that becomes more important for greater values of  $\beta_6/a_{ho}$  and for more highly excited states.

# Chapter 5

## Conclusions

### 5.1 Atoms in a trap

In conclusion, we have presented a VMC formulation for the universal equations of state at the length scale  $\beta_6$  for  $N$  Bose atoms in a symmetric harmonic trap. We have also shown that atoms under strong confinement have significant long-range correlation of the form of  $(r_{ij}/d)^\gamma$ . Since an independent-particle model, such as the Hartree-Fock approximation, corresponds to a variational method based on a wave function with  $F \approx 1$ , the fact that  $F$ , for atoms under strong confinement, deviates significantly from 1 everywhere implies that any independent-particle model is likely to fail for such systems. The results for  $N = 3$  and 5 provide a quantitative understanding of the shape-dependent confinement correction, which is important for a small number of particles under strong confinement [33].

The results provide important insight into the differences in behaviour between atoms which have positive and negative scattering lengths. In the case of  $a_0 > 0$  it was

found that the condensate was stable for large scattering lengths and the long-range correlation

$$F(r) = \left(\frac{r}{d}\right)^\gamma \quad r > d, \quad (5.1)$$

is of great significance in the wavefunction. This is displayed by Figures (4-5) and (4-6). However, in the case of  $a_0 < 0$  it was found that it is not possible to obtain results for large scattering lengths and the variational parameter associated with the long range correlation,  $\gamma$ , is of little significance. For a large number of atoms, attractive interactions are known to decay when the number of bosons is less than a critical value,  $N_c$ . The condensate decays due to negative pressure which is formed at the centre of the trap. When the number of atoms  $N$  exceeds the critical value the Gross-Pitaevskii (GP) equation predicts the system will rapidly collapse. The atomic interactions can be stabilised by the zero point kinetic energy due to the trapping potential, provided the number of atoms does not exceed the critical value [41, 42].

$$N_c = \kappa \left| \frac{a_{ho}}{a_0} \right| \quad (5.2)$$

where  $\kappa$  is the dimensionless average coupling constant, perturbation theory predicts  $\kappa = 0.418$  for spherical traps. If one were to select values for Eq. (5.2), with  $\kappa = 0.5$  and  $N_c = 5$  then we obtain a value of  $\frac{a_0}{a_{ho}} \sim 0.1$ . This value is approximately the same value on Figure 4-10 at which the energy per particle approaches a constant value, this suggests that many-body behaviour is being observed. Further investigation is required for few and many atomic systems with negative scattering length. The aim

of this would be to gain further evidence of many-body behaviour by introducing more than five atoms in a trap. Also both Figures 4-9 and 4-10 display a limit in the scattering length beyond which it was not possible to obtain good results. Our expectation is that as the scattering length is increased the imaginary part of the energy starts to grow until you get to a point at which you are no longer dealing with a stationary state.

## 5.2 Homogeneous Bose Gas

The homogeneous Bose gas was created with  $N = 256$  Bose particles. It was found that for a range of scattering lengths and a density,  $0 \leq \rho_s \leq 1$  the VMVMC results agreed exceptionally well with the nearest-neighbor results. However, for densities of  $\rho_s > 1$ , the VMVMC result did not perform well. Although it is possible to obtain nearest-neighbor theory (NNT) results for this system at higher densities the VMVMC result was not satisfactory which suggests that the wavefunction that was chosen was not adequate to represent this system.

## 5.3 Excited States

The VMVMC method was also applied to s-wave excited states of two interacting trapped atoms. The method was applied to the ground and first two excited states. The results displayed an excellent agreement with the QDT (exact) result for this system. This clearly demonstrates that the VMVMC method may be successfully

applied to excited states of a many Bose-atom system with a high degree of confidence in the results.

## 5.4 Further Work

This project has successfully demonstrated the use of the VMVMC method in describing many Bose atom systems. This is a significant improvement upon previous work which concentrated on treating atoms as hard-spheres.

In order to carry this work into the future a few interesting directions can be explored.

1. Generalize the method in order to incorporate Fermions as well Bose systems
2. Investigate molecular states
3. Incorporate three-body interactions into the wavefunction
4. Investigate cylindrical shaped traps

# Appendix A

## VMVMC Class Structure

The VMVMC algorithm may be composed in any high performance language such as Perl, C++, Java, FORTRAN to name a few. However, it is my recommendation that the algorithm be composed in a language which is capable of supporting object-oriented analysis and design. The main feature of the algorithm is the VMC method which computes  $\delta E$ . The minimization algorithm searches a multi-dimensional space of variational parameters in order to find the minimum  $E$ .

The algorithm has a minimization class which has a dependency on the sub-class *Delta<sub>E</sub>*. *Delta<sub>E</sub>* itself is composed of the local energy and the square of the local energy. The local energy itself and its square are in turn calculated via the Variational Monte Carlo method. The user would be required to provide the following parameters:

1. Number of particles,  $N$ .
2. Number of variational parameters and their respective range.
3. Scattering length,  $a_0$ .

4. Harmonic Oscillator length,  $a_{ho}$  (for trapped atoms)
5. Strength of interaction potential,  $\beta_6$ .
6. Maximum variance,  $\Delta E$ .

In my algorithm the upper limit for an acceptable variance was chosen to be  $1.0 \times 10^{-2}$ , above this limit the quality of the result may be brought into question. Obviously an ideal value for of  $\Delta E = 0$  would be the preferred choice, it was possible in some cases to obtain results where the variance was found to be  $\Delta E \sim 10^{-5}$ .

# Appendix B

## Data Tables

### B.1 Hard Spheres In a Trap

Tables B.1, B.2 and B.3 present data for few and many hard spheres in an external trap.

Table B.1: Data of energy per particle, in units of  $\hbar\omega$ , for two hard spheres in a symmetric harmonic trap. The number in the parenthesis represents the variance in the last digit.

$a_0/a_{ho}$	HS[1]	VMC	$a_0/a_{ho}$	HS[1]	VMC
0.00433	1.5017	1.5022(3)	0.43300	1.6915	1.696(5)
0.04330	1.5174	1.517(9)	0.64950	1.8012	1.806(2)
0.08660	1.5352	1.540(2)	0.86600	1.9209	1.925(9)
0.12990	1.5536	1.558(6)	1.29900	2.1901	2.195(1)
0.17320	1.5719	1.576(9)	1.73200	2.4999	2.50(4)
0.21650	1.5917	1.596(7)	2.16500	2.8511	2.85(6)

Table B.2: Data of energy per particle, in units of  $\hbar\omega$ , for three and five hard spheres in a symmetric harmonic trap. The number in the parenthesis represents the variance in the last digit.

$a_0/a_{ho}$	HS[1] ( $N = 3$ )	VMC ( $N = 3$ )	HS[1] ( $N = 5$ )	VMC ( $N = 5$ )
0.00433	1.50345	1.5067(9)	1.50689	1.5069(9)
0.04330	1.53443	1.537(7)	1.56712	1.571(2)
0.08660	1.56880	1.572(1)	1.63134	1.633(4)
0.12990	1.60330	1.606(6)	1.69404	1.698(4)
0.17320	1.63770	1.641(0)	1.75554	1.759(5)
0.21650	1.67230	1.675(6)	1.81684	1.820(8)
0.43300	1.85090	1.854(2)	2.11542	2.119(2)
0.86600	2.23267	2.236(0)	2.71960	2.721(0)
1.29900	2.64333	2.64(6)	3.34760	3.35(0)
1.73200	3.10667	3.11(0)	4.01800	4.02(2)
2.16500	3.60333	3.60(6)	4.74800	4.74(9)
2.59800	4.15433	4.15(6)	5.56020	5.56(4)

Table B.3: Data of energy per particle, in units of  $\hbar\omega$ , for ten and twenty hard spheres in a symmetric harmonic trap. The number in the parenthesis represents the variance in the last digit.

$a_0/a_{ho}$	HS[1] ( $N = 10$ )	VMC ( $N = 10$ )	HS[1] ( $N = 20$ )	VMC ( $N = 20$ )
0.00433	1.51537	1.53037	1.53203	1.5353(1)
0.04330	1.64246	1.65746	1.77350	1.778(2)
0.08660	1.76977	1.78477	1.99300	1.995(1)
0.12990	1.88628	1.90128	2.18800	2.189(5)
0.17320	1.99959	2.01459	2.36950	2.369(9)
0.21650	2.10739	2.12239	2.54200	2.54(9)
0.43300	2.62162	2.64162	3.34500	3.35(5)
0.86600	3.68260	3.70260	4.91000	4.91(7)

Table B.4: Data of energy per particle for a homogeneous Bose gas, in units of  $\hbar^2/2ma^2$ . The number in the parenthesis represents the variance in the last digit.

$na^3$	E/N (DMC)[2]	E/N (VMC)
$10^{-6}$	$1.262(1) \times 10^{-5}$	$1.262(2) \times 10^{-5}$
$5 \times 10^{-6}$	$6.343(1) \times 10^{-5}$	$6.343(3) \times 10^{-5}$
$10^{-5}$	$1.274(1) \times 10^{-4}$	$1.274(1) \times 10^{-4}$
$5 \times 10^{-5}$	$6.469(3) \times 10^{-4}$	$6.469(4) \times 10^{-4}$
$10^{-4}$	$1.311(1) \times 10^{-3}$	$1.311(1) \times 10^{-3}$
$5 \times 10^{-4}$	$6.880(4) \times 10^{-3}$	$6.880(5) \times 10^{-3}$
$10^{-3}$	$1.424(2) \times 10^{-2}$	$1.424(3) \times 10^{-2}$
$5 \times 10^{-3}$	$8.154(6) \times 10^{-2}$	$8.154(9) \times 10^{-2}$
$10^{-2}$	$1.796(1) \times 10^{-1}$	$1.79(9) \times 10^{-1}$
$5 \times 10^{-2}$	1.338(1)	1.33(7)
$10^{-1}$	3.626(7)	3.62(8)

## B.2 Atoms in a Trap

### B.2.1 Positive scattering length

Repulsive interactions are given by  $a_0 > 0$ , tables B.5 and B.6 tabulate the energy per particle for  $N = 3$  and  $N = 5$  atoms in a spherical trap. Tables B.7 and B.8 present data for the variational parameter  $\gamma$ .

### B.2.2 Negative scattering length

Table B.5: Data of energy per particle, in units of  $\hbar\omega$ , for three atoms in a symmetric harmonic trap. The number in the parenthesis represents the variance in the last digit.

$a_0/a_{ho}$	DMC[1]	$\beta_6/a_{ho} = 0.001$	$\beta_6/a_{ho} = 0.01$	$\beta_6/a_{ho} = 0.1$
0.00433	1.50345	1.5043(1)	1.504(3)	1.505(5)
0.04330	1.53443	1.537(4)	1.545(3)	1.56(6)
0.08660	1.56880	1.567(9)	1.580(4)	1.60(9)
0.12990	1.60330	1.60(3)	1.62(4)	1.65(9)
0.17320	1.63770	1.63(8)	1.66(6)	1.69(8)
0.21650	1.67230	1.67(6)	1.71(1)	1.73(9)
0.43300	1.85090	1.85(1)	1.91(1)	1.95(7)
0.86600	2.23267	2.23(6)	2.32(7)	2.41(1)
1.29900	2.64333	2.64(4)	2.74(9)	2.87(2)
1.73200	3.10667	3.10(9)	3.23(4)	3.37(5)
2.16500	3.60333	3.60(5)	3.73(5)	3.86(9)
2.59800	4.15433	4.16(1)	4.30(1)	4.42(6)
3.03100	4.76200	4.76(3)	4.89(9)	5.018(4)

Table B.6: Data of energy per particle, in units of  $\hbar\omega$ , for five atoms in a symmetric harmonic trap. The number in the parenthesis represents the variance in the last digit.

$a_0/a_{ho}$	DMC[1]	$\beta_6/a_{ho} = 0.001$	$\beta_6/a_{ho} = 0.01$	$\beta_6/a_{ho} = 0.1$
0.004330	1.506886	1.509(5)	1.520(1)	1.53(2)
0.043300	1.567120	1.56(7)	1.58(3)	1.61(6)
0.086600	1.631340	1.63(8)	1.65(9)	1.68(9)
0.129900	1.694040	1.69(6)	1.72(1)	1.75(7)
0.173200	1.755540	1.75(5)	1.78(5)	1.82(4)
0.216500	1.816840	1.81(6)	1.84(7)	1.89(0)
0.433000	2.115420	2.11(5)	2.15(8)	2.20(9)
0.866000	2.719600	2.72(2)	2.79(0)	2.84(4)
1.299000	3.347600	3.34(7)	3.43(0)	3.49(7)
1.732000	4.018000	4.01(9)	4.10(0)	4.16(2)
2.165000	4.748000	4.74(8)	4.83(2)	4.89(9)
2.598000	5.560200	5.56(0)	5.65(6)	5.72(9)

Table B.7: Values of the variational parameter  $\gamma$ , from Eq.( 3.17) for three particles in a symmetric harmonic trap.

$a_0/a_{ho}$	$\beta_6/a_{ho} = 0.001$	$\beta_6/a_{ho} = 0.01$	$\beta_6/a_{ho} = 0.1$
0.00433	0	0.01	0.02
0.04330	0.04	0.05	0.08
0.08660	0.07	0.08	0.12
0.12990	0.1	0.12	0.17
0.17320	0.14	0.17	0.22
0.21650	0.18	0.21	0.26
0.43300	0.36	0.41	0.49
0.86600	0.74	0.83	0.95
1.29900	1.14	1.25	1.38
1.73200	1.61	1.73	1.89
2.16500	2.11	2.24	2.38
2.59800	2.66	2.8	2.95
3.03100	3.26	3.4	3.55

Table B.8: Values of the variational parameter  $\gamma$ , from Eq.( 3.17) for five particles in a symmetric harmonic trap.

$a_0/a_{ho}$	$\beta_6/a_{ho} = 0.001$	$\beta_6/a_{ho} = 0.01$	$\beta_6/a_{ho} = 0.1$
0.00433	0.01	0.02	0.03
0.04330	0.07	0.08	0.12
0.08660	0.14	0.16	0.19
0.12990	0.21	0.23	0.26
0.17320	0.26	0.29	0.33
0.21650	0.32	0.35	0.4
0.43300	0.61	0.66	0.71
0.86600	1.23	1.31	1.35
1.29900	1.85	1.95	2.03
1.73200	2.52	2.63	2.73
2.16500	3.25	3.4	3.5
2.59800	4.1	4.26	4.38

Table B.9: Negative scattering length data of energy per particle, in units of  $\hbar\omega$ , for three atoms in a symmetric harmonic trap. The number in the parenthesis represents the variance in the last digit.

$a_0/a_{ho}$	$\beta_6/a_{ho} = 0.001$	$\beta_6/a_{ho} = 0.1$
-0.001	1.498(6)	1.498(6)
-0.005	1.495(6)	1.495(7)
-0.01	1.49(1)	1.49(1)
-0.05	1.43(1)	1.43(6)
-0.1	1.43(3)	1.44(0)
-0.2	1.39(9)	1.41(5)
-0.3	1.37(0)	1.38(9)
-0.4	1.34(0)	1.37(0)
-0.5	1.32(4)	1.35(8)
-1.0	1.30(6)	1.33(5)
-1.5	1.30(2)	1.33(1)

Table B.10: Negative scattering length data of energy per particle, in units of  $\hbar\omega$ , for five atoms in a symmetric harmonic trap. The number in the parenthesis represents the variance in the last digit.

$a_0/a_{ho}$	$\beta_6/a_{ho} = 0.001$	$\beta_6/a_{ho} = 0.1$
-0.005	1.495(9)	1.496(1)
-0.01	1.48(9)	1.49(1)
-0.05	1.46(6)	1.46(9)
-0.1	1.41(0)	1.41(5)
-0.25	1.39(5)	1.39(9)
-0.5	1.39(1)	1.39(5)
-1.0	1.38(7)	1.39(3)

# Appendix C

## Further Comments on Implementation

We make a few additional comments here on the computational procedure leading to the universal equation of state at length scale  $\beta_6$ , as it is slightly different depending on whether one has the capability of computing the reference functions  $f_{\lambda_s l}^{c(6)}$  and  $g_{\lambda_s l}^{c(6)}$ .

Mathematically, the universal equation of state is rigorously defined using the method of effective potential, in a limit that eliminates all length scales shorter than  $\beta_6$  [11]. The short range behavior of the effective potential is not important, provided that it is sufficiently repulsive and gives rise to the desired  $K^c$ , or  $a_0/\beta_6$ , which are related to each other by Eq. (4.36). For most purposes, the most conveniently effective potential is simply a hard sphere with an attractive tail (HST):

$$v_{\text{eff}}(r) = v_{\text{HST}}(r) = \begin{cases} \infty & , \quad r \leq r_0 \\ -C_6/r^6 & , \quad r > r_0 \end{cases} , \quad (\text{C.1})$$

for which the scattering length, the short-range  $K^c$  parameter, and the number of bound levels for any partial wave  $l$ , can all be found analytically [30].

With this choice of effective potential, the limit that eliminates all length scales shorter than  $\beta_6$  is denoted by  $r_0 \rightarrow 0+$ , and defined as  $r_0$  taking on a *discrete set* of successively smaller, but never zero, values [11]. The corresponding effective potentials all have the same  $K^c$  or  $a_0/\beta_6$ , with the only difference being that the ones with smaller  $r_0$  support a greater number of bound states [30]. Figure C-1 illustrates this limiting process, and shows how the energy per particle for a three-atom system becomes independent of  $r_0$  in the limit of  $r_0 \rightarrow 0+$ , which is equivalent to the limit of a large number of  $s$  wave bound states. Numerically, this limit is simply realized by taking a  $r_0$  that is sufficiently small that the energy has become independent of  $r_0$ .

For each set of parameters  $a_0/a_{ho}$  and  $\beta_6/a_{ho}$ , their ratio determines a parameter  $a_0/\beta_6$ . Without the capability for computing the reference functions  $f_{\lambda_s l}^{c(6)}$  and  $g_{\lambda_s l}^{c(6)}$ , one would proceed to pick a sufficiently small  $r_0/\beta_6$ , either by using the analytic results of Ref. [30] or numerically, such that the effective potential yields the desired  $a_0/\beta_6$ . The correlation function is then found by integrating Eq. (4.32) with  $v$  replaced by the effective potential and matching to the outer behavior at  $d$ , which is typically of the order of  $a_{ho}$  for few atoms in a trap.

For people with the capability of computing the reference functions  $f_{\lambda_s l}^{c(6)}$  and  $g_{\lambda_s l}^{c(6)}$ , no integration of Eq. (4.32) is necessary, as its solution is simply given by Eq. (4.35) with  $K^c$  determined from  $a_0/\beta_6$  by Eq. (4.36). There is also a greater freedom in picking  $r_0/\beta_6$ . It has to be sufficiently small, but it no longer has to be determined from  $a_0/\beta_6$ , because the correlation function is determined from  $a_0/\beta_6$  directly, not

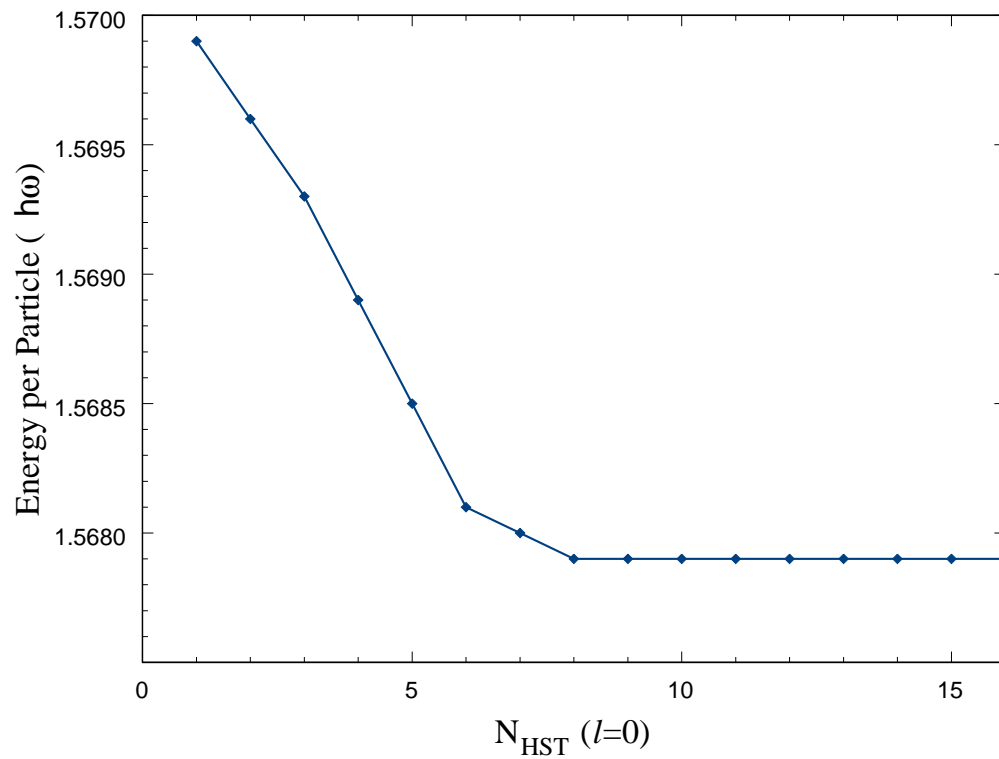


Figure C-1: Energy per particle for three atoms in a trap, with  $a_0/a_{ho} = 0.0866$  and  $\beta_6/a_{ho} = 0.001$ , as a function of the number of  $s$  wave bound states supported by a HST effective potential.

through  $r_0/\beta_6$  as is the case in the first approach. For sufficiently small  $r_0$ , the possible inconsistency between  $r_0/\beta_6$  and  $a_0/\beta_6$  in such an approach has no computational consequence because the correlation function goes to zero in the limit of small  $r_0$ . Our calculations are carried out using this second approach with a  $r_0$  sufficiently small that the corresponding effective potential supports at least 32  $s$  wave bound states.

# Bibliography

- [1] D. BLUME and C. H. GREENE, *Phys. Rev. A* **63**, 063601 (2001).
- [2] S. GIORGINI, J. BORONAT, and J. CASULLERAS, *Phys. Rev. A* **60**, 5129 (1999).
- [3] Y. CHEN and B. GAO, *Phys. Rev. A* **75**, 053601 (2007).
- [4] B. GAO, *Phys. Rev. A* **62**, 050702(R) (2000).
- [5] B. GAO, *Phys. Rev. A* **64**, 010701(R) (2001).
- [6] B. GAO, *Euro. Phys. J. D* **31**, 283 (2004).
- [7] K. HUANG, *Statistical Mechanics*, John Wiley & Sons, 2nd edition, 1987.
- [8] H. REICHENBACH, *Philosophic Foundations of Quantum Mechanics*, Dover, 1st edition, 1944.
- [9] B. D'ESPAGNAT, *Conceptual Foundations of Quantum Mechanics*, Perseus Books, 2nd edition, 1999.
- [10] J. W. NEGELE and H. ORLAND, *Quantum Many-Particle Systems*, Westview Press, 2nd edition, 1998.

- [11] B. GAO, *J. Phys. B: At. Mol. Opt. Phys.* **37**, L227 (2004).
- [12] I. KHAN and B. GAO, *Phys. Rev. A* **73**, 063619 (2006).
- [13] T. D. LEE and C. N. YANG, *Phys. Rev.* **105**, 1119 (1957).
- [14] T. D. LEE, K. HUANG, and C. N. YANG, *Phys. Rev.* **106**, 1135 (1957).
- [15] M. H. KALOS, D. LEVESQUE, and L. VERLET, *Phys. Rev. A* **9**, 2178 (1974).
- [16] D. M. CEPERLEY, *Rev. Mod. Phys.* **67**, 279 (1995).
- [17] J. L. DUBOIS and H. R. GLYDE, *Phys. Rev. A* **63**, 023602 (2001).
- [18] F. DALFOVO, S. GIORGINI, L. P. PITAEVSKII, and S. STRINGARI, *Rev. Mod. Phys.* **71**, 463 (1999).
- [19] B. GAO, E. TIESINGA, C. J. WILLIAMS, and P. S. JULIENNE, 2005.
- [20] R. RYDBERG, *K. Svensk Vetenskaps Akad. Handlinger* **23**, 1 (1890).
- [21] S. N. BOSE, *Z. Phys* **26**, 178 (1924).
- [22] A. EINSTEIN, *Sitz. Ber. Preuss. Akad. Wiss.(Berlin)* **1**, 3 (1925).
- [23] M. H. ANDERSON *et al.*, *Science* **269**, 198 (1995).
- [24] C. J. PETHICK and H. SMITH, *Bose-Einstein Condensation in Dilute Gases*, Cambridge, 1st edition, 2002.
- [25] R. JASTROW, *Phys. Rev.* **98**, 1479 (1955).
- [26] J. M. THIJSEN, *Computational Physics*, Cambridge University Press, 1999.

- [27] Y. CHEN and B. GAO, *Bull. Am. Phys. Soc.* **50**, 80 (2005).
- [28] D. PINES, *The Many-Body Problem*, Addison-Wesley, 1997.
- [29] A. L. FETTER and J. D. WALECKA, *Quantum Theory of Many-Particle Systems*, Dover, 2003.
- [30] B. GAO, *J. Phys. B: At. Mol. Opt. Phys.* **36**, 2111 (2003).
- [31] B. GAO, *Phys. Rev. A* **58**, 1728 (1998).
- [32] G. F. GRIBAKIN and V. V. FLAMBAUM, *Phys. Rev. A* **48**, 546 (1993).
- [33] H. FU, Y. WANG, and B. GAO, *Phys. Rev. A* **67**, 053612 (2003).
- [34] E. TIESINGA, C. J. WILLIAMS, F. H. MIES, and P. S. JULIENNE, *Phys. Rev. A* **61**, 063416 (2000).
- [35] D. BLUME and C. H. GREENE, *Phys. Rev. A* **65**, 043613 (2002).
- [36] E. L. BOLDA, E. TIESINGA, and P. S. JULIENNE, *Phys. Rev. A* **66**, 013403 (2002).
- [37] H. T. STOOFF *et al.*, *Phys. Rev. A* **74**, 033621 (2006).
- [38] T. BUSCH, B.-G. ENGLERT, K. RZAZEWSKI, and M. WILKENS, *Found. Phys.* **28**, 549 (1998).
- [39] B. GAO, E. TIESINGA, C. J. WILLIAMS, and P. S. JULIENNE, *Phys. Rev. A* **72**, 042719 (2005).

- [40] B. GAO, *Phys. Rev. A* **58**, 4222 (1998).
- [41] V. I. YUKALOV *et al.*, *Phys. Rev. A* **72**, 063611 (2005).
- [42] P. A. RUPRECHT *et al.*, *Phys. Rev. A* **51**, 4704 (1995).